CONFORMATIONAL STUDIES OF SYNTHETIC COPOLYPEPTIDES

A Thesis Submitted to
The Faculty of Science,
Osaka University
by
NOBORU NISHIOKA

1976

CONFORMATIONAL STUDIES OF SYNTHETIC COPOLYPEPTIDES

A Thesis Submitted to

The Faculty of Science,

Osaka University

BY

NOBORU NISHIOKA

1976

Acknowledgments

Contents

Chapter 6. Conformation of Diblock Copolypeptides of
γ-Benzyl D-Glutamate and L-Glutamate
in m-Cresol

Principal Notations and Abbreviations

For the sake of convenience, various notations and abbreviations used are listed below.

Notations

$\bar{N}$ = average degree of polymerization

$\bar{N}_w$ = weight-average degree of polymerization

$\bar{M}_w$ = weight-average molecular weight

$\bar{M}_n$ = number-average molecular weight

$[A]_0/[I]_0$ = molar ratio of NCA to initiator

b_0 = Moffitt parameter

$[\eta]$ = intrinsic viscosity

$\langle \mu^2 \rangle^{1/2}$ = mean-square dipole moment

μ_h = monomeric dipole moment of helix unit

$\tau T/\eta_0$ = mean rotational relaxation time corrected
for solvent viscosity η_0 and absolute
temperature T

f_N = average fraction of helix units

Θ_N = average fraction of intact hydrogen bonds

s = helix-coil equilibrium constant

$\sigma^{1/2}$ = cooperativity parameter for the formation
of helical sequences

Polypeptides

    NCA = N-carboxy α-amino acid anhydride

    BDG = γ-benzyl D-glutamate

    BLG = γ-benzyl L-glutamate

    CBL = ε-carbobenzoxy L-lysine

    LA = L-alanine

    PBDG = poly(BDG)

    PBLG = poly(BLG)

    PCBL = poly(CBL)

    PLA = poly(LA)

    PBLA = poly(β-benzyl L-aspartate)

Solvents

    DCA = dichloroacetic acid

    DMF = dimethylformamide

    DCM = dichloromethane

    EDC = ethylene dichloride

    HFIP = hexafluoroisopropanol

    TFA = trifluoroacetic acid

Measurements

    IR = infrared absorption

    NMR = nuclear magnetic reasonance

    ORD = optical rotatory dispersion

Chapter 1

Introduction

1-1 General Introduction

There are now available high-molecular-weight homopolypeptides of most naturally occurring α-amino acids, copolymers consisting of several amino acid residues in random sequences, and copolymers in which a few sequences of amino acids are linked in block. Furthermore, in recent years, progress has been made in the synthesis of sequential polypeptides which consist of a known repeat sequence of a few kinds of amino acids. The availability of such a variety of synthetic polypeptides has made it possible to investigate their physical properties in more detail and to utilize them more widely as model substances for proteins.[1-4] For protein chemists, who are primarily interested in the correlation between structure and function of the proteins, conformations and biological activities of synthetic polypeptides in aqueous solution must be the subjects of considerable attraction. On the other hand, polymer physical chemists may find synthetic polypeptides very attractive from the fact that this kind of polymers takes different chain conformations in solution, such as α-helix, β-form, and random coil, depending on the

environmental conditions.

Since the discovery by Doty and collaborators,[5-7] the helix-coil transition of polypeptides in solution has been investigated on a number of systems. Theoretical and experimental advance in this field of study may be found in several recent review articles.[8-16] According to statistical mechanical theories,[17-22] the helical fraction of a polypeptide molecule in dilute solution is determined by three parameters N, s, and σ. Here N is the degree of polymerization of the molecule, s the equilibrium constant for the helix formation, and σ the helix-initiation parameter. The theories predict that in the helix-coil transition region a polypeptide molecule consists of an alternating array of helical and random coil sequences, which is often called an interrupted helix, and that the frequency of alternation depends on σ. If experimental data for helical fraction are available as a function of molecular weight, the transition parameters s and σ can be evaluated by analyzing such data in terms of an appropriate theory,[23] e.g., that of Zimm and Bragg.[17] Besides the helical fraction, there are also available theoretical expressions[22,24-26] for such average quantities of interrupted helix as the mean-square radius of gyration, the mean-square end-to-end distance, the alternating

-2-

frequency of helical and random coil sequences, and so forth, all of which are expressed in terms of the three parameters N, s, and σ. Thus the transition parameters s and σ, once evaluated experimentally, allow one to compute the average conformational characteristics of a given polypeptide in sufficient detail.[27,28] It is known that the helix-coil transition behavior of polypeptides depends greatly on the solvent condition as well as on the structure of polypeptides, and this fact has been interpreted successfully in terms of the effect of solvent conditions on the transition parameters.[29-32]

Most of these investigations have been concerned with homopolypeptides, and those on copolypeptides are still meager in spite of their importance relative to the protein structure.[12,13,33-40] This may be attributed to the lack of appropriate model system and relevent theories to analyze their transition data. However, one may not overlook the significance of the contributions by Scheraga and collaborators[12,13,36,39,40] to the statistical mechanical theories of random copolypeptides. These authors have developed a method called "host-guest technique" to analyze helix-coil transition curves of random copolypeptides which consist of one kind of amino residue (guest) randomly incorporated into the polymer of the other residue (host).[39]

This method allows the transition parameters of the guest residue to be estimated if those for the host residue are known in advance, and actually it has been applied to a number of naturally occurring amino acids in water, the homopolypeptides of which are insoluble in water.[41-47]

In this thesis, we shall chiefly be concerned with block copolypeptides: the reason is two-fold.

Firstly, the arrangement of amino acid residues in a polypeptide chain is one of the important factors for its helix stability because at least three consecutive residues have to be distorted simultaneously in order that an α-helical turn may be formed and stabilized by one intrachain hydrogen bond.[48] Copolypeptides consisting of a few blocks of amino acid residues may be the simplest of the model systems for investigating the effect of this factor on the helix stability. However, no such attempt has yet been reported.

Secondly, we have recently developed a procedure for synthesizing and characterizing block copolypeptides of known sequences with moderate chain lengths.[49] Thus if a block copolypeptide of a few amino acid residues, whose homopolypeptides are well characterized in the statistical-mechanical terms, is chosen as a sample, comparison of its helix-coil transition behavior with those of the parent

homopolypeptides will provide information about the effect
of residue arrangement on the helix stability.

Poly(L-alanine) (PLA) is the simplest α-helix-forming
polypeptide, having only one methyl group as the side chain.
For this structural simplicity as well as its importance
in the protein structure, it has been subjected to a
number of investigations, although its insolubility in
ordinary organic solvents and in aqueous media have greatly
hampered the conformational studies. Gratzer and Doty[50]
developed an ingeneous means called "block copolymer
technique", in which a non-polar polypeptide was sandwiched
between blocks of water-soluble D,L-polypeptide. The
present study will utilize a similar idea for studying the
chain conformation of PLA in organic solvent systems.

1-2 Purposes and Scope of This Work

This thesis concerns itself with conformations of
block copolypeptides composed of two kinds of helix-forming
peptide residues. Attention is paid to explore how the
helix formation of the one of the constituent residues is
 influenced by the presence of the other. Block
copolypeptides synthesized for this purpose were of the
types: BLG-CBL, BLG-CBL-BLG, BLG-LA, BLG-LA-BLG, and
BLG-BDG, where BLG = γ-benzyl L-glutamate, BDG = γ-benzyl

D-glutamate, CBL = ε-carbobenzoxy L-lysine, and LA = L-alanine. Optical rotatory dispersion (ORD), dielectric dispersion, infrared absorption (IR), and intrinsic viscosity ([η]) were used to estimate the molecular conformation and shape of the copolypeptides.

Chapter 2 summarizes the principal experimental methods employed throughout this work.

Chapter 3 deals with the conformations of block copolypeptides consisting of BLG and CBL in m-cresol. This choice of solvent has been made because PCBL undergoes a thermally-induced helix-coil transition in m-cresol around 25°C but PBLG forms a stable α-helix under the same solvent condition.

Chapter 4 is concerned with helix-coil transitions of BLG-CBL-BLG block copolypeptides in mixtures of dichloro-acetic acid (DCA) and ethylene dichloride (EDC). Nagai's theory[22] of helix-coil transition in homopolypeptide is extended to block copolypeptides and applied to ORD data for the BLG-CBL-BLG copolypeptides.

In chapter 5, the conformation of block copolypeptides consisting of BLG and LA is discussed. Owing to the absence of polar side chain, PLA hardly dissolves in usual organic solvents. However, block copolypeptides of LA and BLG were found to be soluble in many organic solvents.

The dipole moment of peptide backbone is estimated and
the side chain effect on it is discussed with the aid of
available data for other polypeptides.

Chapter 6 is devoted to diblock copolypeptides of the
type BDG-BLG. If each of the two blocks maintains its
intrinsic helical sense, the block copolypeptide should
form a once-broken rod. ORD, dielectric dispersion, and
viscosity data were used to test this possibility and the
conformational induction effect between the D and L
residues is discussed.

Chapter 2

Experimental Methods

This chapter describes the principal experimental methods employed throughout the present study. The specific details of each method are deferred to the respective chapters.

2-1 Solvents

Dichloroacetic acid (DCA) was distilled twice with concentrated sulfuric acid under reduced nitrogen atmosphere, bp 50 - 55°C (1 - 2 mm). N,N-Dimethylformamide (DMF) was dried with $BaSO_4$ or BaO, and distilled under reduced nitrogen atmosphere over BaO, bp 37 - 40°C (8 - 10 mm). m-Cresol was distilled under nitrogen atmosphere over P_2O_5, bp 55 - 60°C (1 - 2 mm). Trifluoroacetic acid (TFA) was fractionally distilled over P_2O_5, bp 68.4 - 69.4°C. Hexafluoroisopropanol (HFIP) was fractionally distilled over CaO, bp 56 - 57°C. Other solvents were thoroughly purified according to the standard procedures and fractionally distilled. All the solvents were used immediately after distillation.

2-2 N-Carboxy α-Amino Acid Anhydride

γ-Benzyl L-glutamate (BLG) and γ-benzyl D-glutamate

(BDG) were converted to the respective N-carboxy anhydrides (NCA) by the method of Blout and Karlson.[51] A weighed amount of glutamate crushed to powder and dried in vacuum was suspended in tetrahydrofuran and then phosgen gas was bubbled through at 40 - 45°C. After several hr a clear, pale yellow solution was obtained. This solution was concentrated under reduced pressure and diluted with chloroform, and to it was added n-hexane slowly until the NCA began to crystallize. The NCA thus obtained was purified by repeated crystallization under nitrogen atmosphere from an ethyl acetate solution with n-hexane as a precipitant.

ε,N-Carbobenzoxy L-lysine-N-carboxy anhydride (CBL-NCA) was prepared from ε-carbobenzoxy L-lysine according to Fasman et al.,[52] except that tetrahydrofuran, instead of ethyl acetate, was used as solvent. The technique was actually identical with that described above.

L-Alanine-N-carboxy anhydride (LA-NCA) was prepared from L-alanine by the method described above with isopropyl ether being used as a solvent for recrystallization.

2-3 Polymerization Kinetics

The polymerization of NCA is generally considered to consist of a repetitive, stepwise addition of peptide units

with the simultaneous expulsion of carbon dioxide.[1] The

evolution of CO_2 gas provides a convenient means to

follow the progress of this reaction. We used the method

of Lundberg and Doty[53] to study the polymerization

process.

A weighed amount of NCA was dissolved in DMF and

mixed with a DMF solution of initiator in a reaction tube

of about 2ml capacity, and the CO_2 gas evolved as the

result of polymerization was swept out by a stream of dry

Ar gas and absorbed into an 0.04N $Ba(OH)_2$ solution placed

in a conductance cell. The change in conductance of the

solution was followed by Kohlrausch bridge, and from the

data the amount of NCA consumed was calculated according

to the expressions:

$$[CO_2]_t = (V/2)(C_0 - C_t) = (500KV/\Lambda)(1/R_0 - 1/R_t)$$

$$\text{(2-1)}$$

$$[A]_t = [A]_0 - [CO_2]_t \qquad \text{(2-2)}$$

where the subscripts 0 and t denote the values of each

quantity at time t=0 and t, respectively. $[CO_2]_t$ is the

number of moles of CO_2 absorbed at time t, C_0 and C_t are

the concentrations of the $Ba(OH)_2$ solution in equiv./l,

R_0 and R_t are the values for the resistance of the $Ba(OH)_2$

-10-

solution, K is the conductivity cell constant (K = 0.409 cm^{-1}), V is the volume of the $Ba(OH)_2$ solution in liter (V = 0.025), Λ is the equivalent conductance of $Ba(OH)_2$, and $[A]_0$ and $[A]_t$ are the numbers of moles of NCA in the reaction tube. Complete absorption of the evolved CO_2 was effected by adding 0.5 % of 1-butanol to the $Ba(OH)_2$ solution. The $Ba(OH)_2$ solution was standardized against known amounts of CO_2 evolved from the permanganate-oxalic acid reaction. The initial concentration of NCA was fixed at about 0.22 mol/l and the molar ratio of NCA to initiator $[A]_0/[I]_0$ was 10.

2-4 Molecular Weight Determinations

Weight-average molecular weights $\overline{M}_w$ were determined by the sedimentation equilibrium method with DMF or HFIP of 25°C as solvents. Use was made of a Beckman-Spinco Model E analytical ultracentrifuge equipped with the Rayleigh interference optical system and a Kel-F coated 12 mm double-sector cell. The following equations were used for data analysis.[54]

$$1/M_{app} = 1/\overline{M}_w + 2A_2(C_a + C_b)/2 \qquad (2-3)$$

with M_{app} defined by

-11-

$$M_{app} = [2RT/(1 - \overline{v}\rho)\omega^2](C_b - C_a)/(r_b^2 - r_a^2)C_0$$

$$(2-4)$$

where C_0 is the initial solute concentration, C_a and C_b are the concentrations at sedimentation equilibrium at the meniscus and the cell bottom, respectively, r_a and r_b are the radial distances from the center of rotation to the meniscus and the bottom, respectively, ρ is the density of the solvent, $\overline{v}$ is the partial specific volume of the solute, ω is the angular velocity of the rotor, A_2 is the second virial coefficient, R is the gas constant, and T is the absolute temperature.

The values for $\overline{v}$ of BLG-CBL-BLG polymers were estimated from those of pure PBLG and PCBL, i.e., 0.786[55,56] and 0.803 ml/g,[57] with the assumption that they were linearly related to the weight fraction of BLG. Fragmental data for triblock copolypeptides supported this assumption. The same value of 0.117 ml/g had been reported for the specific refractive index increments (dn/dc) at 546 nm of both PBLG and PCBL in DMF.[56,57] Hence this value was taken to be appropriate for BLG-CBL-BLG copolypeptides. For BLG-LA-BLG copolypeptides, the $\overline{v}$ in DMF and in HFIP were determined from the density data obtained by using bicapillary pycnometers, and their

Table 2-1 Partial specific volume $\bar{v}$ and specific
refractive index increments (dn/dc) of
block copolypeptides in DMF and HFIP at 25°C

Sample code	LA wt-%[a]	(dn/dc), ml/g		$\bar{v}$, ml/g	
		DMF	HFIP	DMF	HFIP
GAG-1	4.0	0.115_0	–	–	–
GAG-2	4.3	–	–	0.781	–
GAG-3	10.0	0.113_6	0.235	0.774	–
GAG-4	8.5	–	0.235	0.776	–
GAG-5	16.8	–	0.241	–	–
GAG	14.5	–	–	–	0.777
GAG-70	23.7	–	0.249	–	0.778
PBLG		0.117_3	–	0.786	0.773

a. Estimated by elemental analysis.

(dn/dc) at 546 nm were determined by the use of a modified
Schultz-Cantow differential refractometer. The numerical
results obtained are collected in Table 2-1. Figure 2-1
shows that $\bar{v}$ and (dn/dc) are linearly related to the
weight fraction of LA. Values for other copolypeptide
compositions were obtained from these data by either
extrapolation or interpolation.
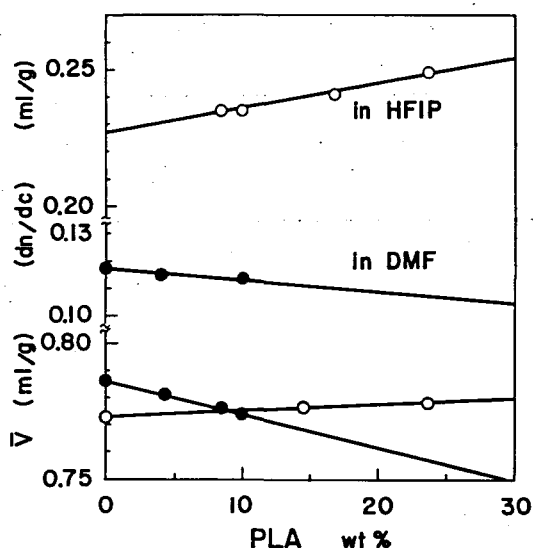
Figure 2-1
Specific refractive index increment (dn/dc) and partial
specific volume v̄ data for copolypeptides in HEIP (O)
and in DMF (●) at 25°C, respectively.

2-5   Dielectric Measurements

A transformer bridge (TR-1C transformer bridge, Ando
Electric Co., Tokyo) was used in conjunction with an HP
3310A Function Generator (Yokogawa-Hewlet-Packard)
operating at frequencies between 0.005 Hz and 5 MHz.
Depending on the frequency range investigated, the
following three detectors were used for null-point
detection: a 1232AP tuned amplifier and null detector

(20 Hz - 20 KHz, General Radio), a tuned amplifier and null detector (20 - 700 KHz, constructed in our laboratory), and a 9R59DS radio receiver (550 KHz - 30 MHz, TRIO). Most of the measurements were performed in a brass concentric cylindrical cell, which had a guard circuit and was assembled with Tefron spacers. The cell was calibrated with benzene and monochlorobenzene as reference liquids, and it had an air capacitance C_0 of 22.85 pF. The temperature of the cell, measured by means of a thermocouple attached to the outer cell wall, was regulated to $\pm$ 0.01°C. Conductance and capacitance readings were taken on both solution and solvent, and the differences between the correponding readings, i.e., the capacitance increment ΔC and the conductance increment G, were used to evaluate the dielectric increment $\Delta\varepsilon'$ and the loss factor $\Delta\varepsilon''$ associated with the solute by means of the equations:

$$\Delta\varepsilon' = \Delta C/C_0 \qquad\qquad G = G_d + \Delta\varepsilon''C_0\omega \qquad (2\text{-}5)$$

where G_d is the dc conductance and $\omega(=2\pi f)$ is the angular fresuency. The value for G at some low frequency, where there was observed no more change in G due to the solute polarization, was taken as that for G_d.

2-6 Optical Rotation Measurements

Optical rotation measurements were performed at various temperatures. A JASCO Model DIP-SL automatic polarimeter with quartz cells of 1 dm path was used at wavelengths of 436, 546, and 578 nm. Optical rotatory dispersions (ORD) were measured in the range of wavelengths from 300 to 600 nm by use of a JASCO ORD/UV-5 recording spectrometer. The data were analyzed in terms of the Moffitt-Yang equation[58] to determine values of the Moffitt parameters a_0 and b_0, with λ_0 taken to be 212 nm

$$[m']_\lambda = a_0\lambda_0^2/(\lambda^2 - \lambda_0^2) + b_0\lambda_0^4/(\lambda^2 - \lambda_0^2)^2 \qquad (2-6)$$

where $[m']_\lambda$ is the mean residue rotation at wavelength λ, a_0 is a constant which is expected to vary with the nature of the sidechain of the polypeptide and to depend on the solvent used, whereas b_0 should be an intrinsic property of the helical skeleton, and b_0 changes its sign if the sense of the helix is changed.

2-7 Viscosity Measurements

Viscosity measurements were made by use of Ubbelohde viscometers designed so that no kinetic energy correction was needed. Data were taken with DCA, DMF, and m-cresol

as solvents and analyzed to determine intrinsic
viscosities by the usual Huggins plots.

2-8 Infrared Absorption Measurements

Oriented films were prepared on KBr plates by
rubbing viscous dioxane solutions with spatula in one
direction until the solvent had been evapolated.
Infrared absorption measurements were taken on the films
thus prepared by means of a JASCO Model DS-402G
spectrometer. The spectral region of 4000 - 400 cm^{-1}
was examined.

Chapter 3

Conformation of Block Copolypeptides of γ-Benzyl L-Glutamate and ε-Carbobenzoxy L-Lysine in m-Cresol

3-1 Introduction

It has been shown that homopolypeptides of γ-benzyl L-glutamate (BLG) residues dissolved in m-cresol assume a stable α-helical conformation,[5,59-61] while those of ε-carbobenzoxy L-lysine (CBL) residues in the same solvent undergo a sharp coil-to-helix transition in the temperature region around 25°C.[57,62-64] In this chapter we describe an experimental investigation of the question as to whether helix formation of the CBL chain is affected if it is incorporated between blocks of helical BLG chains. Figure 3-1 schematically shows predicted conformation of PBLG, PCBL, and a triblock copolypeptide of the type BLG-CBL-BLG in various solvents. Of particular interest is the behavior in m-cresol at low temperature, where PBLG is helical but PCBL is randomly coiled.[5,57,59-64] If there were no helix inducing effect of the flanking BLG blocks, the molecule would take up a once-broken rod shape as shown. The desired triblock copolypeptides with a central CBL block of varying length were prepared by successive polymerization of the corresponding amino acid N-carboxy
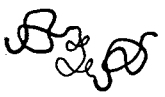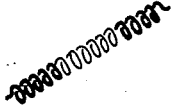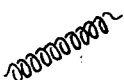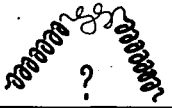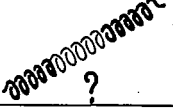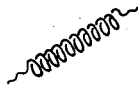
	PBLG	BLG-CBL-BLG	PCBL
DCA			
DMF			
m-cresol (low temp.)		?	
m-cresol (high temp.)		?	

Figure 3-1.
Conformation of PBLG, PCBL, and triblock copolypeptide
BLG-CBL-BLG in various solvents.

anhydride (NCA) with a primary amine as initiator. First,

the kinetic processes of the copolymerization were pursued

inorder to examine whether the procedure used gives

samples of the desired copolypeptide structure. Then,

optical rotatory dispersion, dielectric dispersion, and

intrinsic viscosity were used to estimate the molecular

comformation and shape of the samples in m-cresol at room

temperature. The results revealed an appreciable

conformational induction both in tri-block and di-block

copolypeptides.

3-2 Polypeptide Samples

The preparation of triblock copolypeptides of the type BLG-CBL-BLG was carried out in DMF at room temperature according to the following scheme. First, BLG-NCA was polymerized with n-butylamine as an initiator, with the mole ratio of NCA to initiator fixed at 20. The initial NCA concentration was about 5 % by weight. The process of polymerization was followed by measuring the pressure of CO_2 gas evolved. After about three hr the evolution of CO_2 gas stopped, and an aliquot of the polymerization mixture was transferred to mixture of CBL-NCA and DMF, in which the NCA-initiator mole ratio had been adjusted to a specific value. After the polymerization initiated by the aliquot had been continued for six hr, a weighed amount of BLG-NCA dissolved in DMF was added, and the polymerization mixture was allowed to stand overnight with stirring. The final mixture was poured into a large volume of methanol, and the polypeptide precipitated was collected and freeze-dried from dioxane solution. In this way, five samples were prepared, which were expected to contain a CBL block of desired length (5 to 60 residues) between two BLG blocks, each consisting of about 20 residues. Another sample of

the structure BLG-CBL was prepared in a similar way.

According to well-established evidence,[51,53,65-68] the amino acid residue at the growing end of each preformed polypeptide chain maintains activity so that it can initiate polymerization of newly added NCA. Thus, during the period of standing, a polypeptide chain should grow from one end of the each preformed polypeptide chain to form a block copolypeptide. The length of the blocks depend on the mole ratio of NCA to initiator under the assumption described above.

The triblock copolypeptide samples were fractionated by the column elution method with mixtures of methanol and dichloromethane as eluent, and the appropriate middle fractions were chosen for measurements. These fractionation data indicated that the original samples had relatively narrow distributions in both molecular weight and composition. Table 3-1 summarizes the preparative data. The amino acid compositions of the block copolypeptides were determined by elemental analysis. The weight-average molecular weights of the fractionated samples were determined by the sedimentation equilibrium method, with the results given in Table 3-2.

Table 3-1. Preparative data for block copolypeptides

Sample code	$[A]_0/[I]_0$ [a]	$\bar{M}_v \times 10^{-4}$ [b]	$\bar{N}_v$	CBL [c] mole %	Yield %
GLG-1	20-5-20	1.05	46.9	11.5	86
GLG-2	20-10-20	1.18	52.0	18.5	83
GLG-3	20-20-20	1.32	56.9	29.9	82
GLG-4	20-40-20	1.75	73.2	46.3	87
GLG-5	20-60-20	2.30	94.4	57.5	87
GL-6	20-20	1.12	46.9	45.9	71

a. Mole ratio of NCA to initiator.
b. Calculated from intrinsic viscosities in DCA at $25^{\circ}C$, $[\eta]_{DCA}$, using an empirical relation between $[\eta]_{DCA}$ and $\bar{M}_w$ for the block copolypeptides shown in Figure 3-8.
c. Estimated by elemental analysis.

3-3 Reaction Kinetics

Polymerization of NCA initiated with a primary amine usually follows a first-order reaction scheme represented by[51,65-68]

$$\log ([A]_0/[A]_t) = 0.434[I]_0 k_2 t \qquad (3-1)$$

where $[I]_0$ is the molar concentration of initiator at time $t = 0$ and k_2 is the rate constant for the propagation step

Table 3-2. Molecular weights of fractionated
block copolypeptides

Sample code	$\bar{M}_w \times 10^{-4}$	$A_2 \times 10^4$ mol ml/g^2	CBL mol %	$\bar{N}_w{}^a$	$\bar{N}_G{}^b$	$\bar{N}_L{}^c$
GLG-12	1.31	8.1	11.3	58.5	51.9	6.6
GLG-22	1.39	6.9	18.8	61.1	49.6	11.5
GLG-331	1.64	6.3	28.5	71.0	50.8	20.2
GLG-42	1.79	6.2	45.9	74.9	40.5	34.4
GLG-52	2.16	5.0	58.9	88.5	36.4	52.1
GL-6	1.34	6.7	45.9	56.1	30.4	25.7

a. Weight-average degree of polymerization.
b. Average degree of polymerization of BLG residues.
c. Average degree of polymerization of CBL residues.

in liter/mol sec. This equation can be transformed to the
statement that plots of $\log([A]_0/[A]_t)$ versus t follow a
straight line passing through the origin and that, with
the value of $[I]_0$ known separately, one can evaluate k_2
from the slope of the line. Equation (3-1) holds when the
initiation step is much faster than the propagation step,
and moreover, the latter proceeds without termination.
If such an ideal reaction mechanism is obeyed, the product
should have a narrow molecular weight distribution

represented by Poisson's formula, and the number-average degree of polymerization should be equal to $[A]_0/[I]_0$. In fact, it was found[49,53,65] that polymerization of BLG-NCA in DMF typically obeyed this ideal reaction mechanism, and the finding was successfully used to synthesize once-broken rod polypeptides[49,61] and DL block copolypeptides[49] of narrow molecular weight distribution. These studies suggest that use of DMF as solvent together with a primary amine as initiator was crucial for realization of the ideal reaction mechanism: polymerization of BLG-NCA in dioxane was shown to follow a two-stage reaction mechanism[53,65] and to yield a very broad distribution of molecular weight. Therefore, the present copolymerization was carried out with DMF as solvent and n-butylamine as initiator, with the expectation that the sample should have a sequence length distribution close to that computed from the $[A]_0/[I]_0$ values taken at the three steps of the copolymerization. The following data confirm this expectation.

Figure 3-2 illustrates typical kinetic data for the case in which $[A]_0/[I]_0 = 10$ at each of the three stages. It is to be observed that CO_2 gas started evolving immediately after addition of each NCA solution. The three portions of the curve, two for polymerization of BLG-NCA
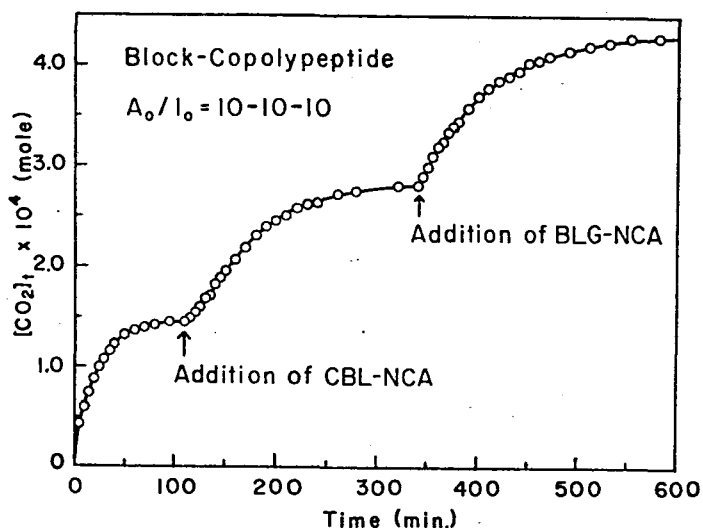
Figure 3-2.
Kinetic curve for block copolymerization of BLG-NCA and
CBL-NCA with initiation by n-butylamine in DMF at $25^{\circ}C$.
The $[I]_0$ at the three stages were 13.3×10^{-3},
6.63×10^{-3}, and 4.63×10^{-3} mol/l, respectively, with
the mole ratios of NCA being fixed at 10.

and one for polymerization of CBL-NCA, are separately

replotted in Figure 3-3 according to Eq. (3-1). For all

the three kinetic processes the experimental data are seen

to obey Eq. (3-1). The polymerization rates for this and

another case in which $[A]_0/[I]_0 = 5$ are given in Table 3-3.

For comparison, homopolymerization of CBL-NCA was carried

out in DMF of $25^{\circ}C$ with n-butylamine as initiator. The

results also conformed to the first-order reaction
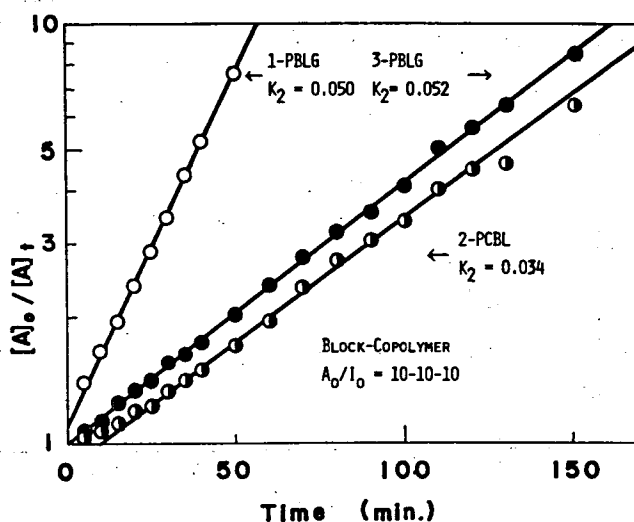
Figure 3-3.
Logarithm of $[A]_0/[A]_t$ plotted versus time with the
data shown in Figure 3-2.

mechanism and yielded the rate constants included in
Table 3-3. Within experimental uncertainty, the rate
constants for CBL-NCA are identical both in the
homopolymerization and in the copolymerization. It is
also seen that the rate constants for the BLG-NCA in the
initial and final steps of the copolymerization are in
substantial agreement with each other. Therefore, a block
copolypeptide synthsized in this way is expected to have
a sequence length distribution corresponding to the
amounts of NCAs that have been fed successively into the

Table 3-3. Polymerization rates of NCAs
in DMF at 25°C

NCA[a]	$[A]_0/[I]_0$	k_2, l/mol sec
BLG-CBL-BLG	10-5-10	0.053-0.038-0.048
BLG-CBL-BLG	10-10-10	0.050-0.034-0.052
CBL	10	0.039
CBL	20	0.049
CBL	30	0.044

a. Polymerized with initiation by n-butylamine
from left to right in the indicated order.

reaction mixtures.

Preparative polymerizations were carried out in a
similar fashion, except that the reaction times were
longer than those for the kinetic experiments. The results
are are summarized in Table 3-1, which, as expected from
the above-mentioned discussion of the kinetic data, shows
that the viscosity-average degree of polymerization of the
samples obtained are in good agreement with the total mole
ratios of NCA to initiator. The mole fractions of CBL
residues determined from elemental analysis also agree
with those calculated from the amounts of the NCAs used.

3-4 Optical Rotatory Dispersion

Table 3-4 lists values of the Moffitt parameters a_0 and b_0 obtained for CBL-BLG copolypeptides. The values of b_0 for the triblock copolypeptides are in the range between -460 and -540 at 20°C and a little larger at 40°C. With the understanding that b_0 is a direct measure of helical fraction, we may conclude for the reason given later that the triblock copolypeptides examined are essentially helical in m-cresol.

As the degree of polymerization N decreases, the b_0 of PBLG in m-cresol shows a systematic increase, starting

Table 3-4. Moffitt parameters for block
copolypeptides in m-cresol

Sample code	$-b_0$		a_0	
	20°C	40°C	20°C	40°C
GLG-12	539	517	362	333
GLG-22	532	513	323	294
GLG-331	513	493	267	243
GLG-42	459	443	158	146
GLG-52	463	466	111	119
GL-6	405	436	158	171

from a value of -630 characteristic of α-helix at very large N and reaching -540 at N = 50 when estimated from available data.[49,60,69] No direct estimation of the b_0 for helical PCBL in m-cresol is feasible, because this polypeptide in m-cresol cannot be brought to a perfect helix in the temperature range accessible to experiment. On the other hand, both PBLG and PCBL become helical in DMF, but the $-b_0$ value of the latter is lower than that of the former by 10 - 15 %.[57] If a similar difference is assumed to exist for m-cresol solution, we may assign a value of -460 for the b_0 of a helical PCBL sample with an N of 50 in m-cresol. Thus the b_0 values for helical triblock copolypeptides with an N of 50 should increase from -540 to -460 as the CBL content increases.

Looking at Table 3-4 with this expectation, one finds that the triblock copolypeptides studied all assume helical conformation in m-cresol at 20 and 40°C. Since the isolated PCBL chains in the same solvent at 20°C are randomly coiled, this finding implies that the flanking helical BLG blocks act to induce helical winding of the central CBL block. Naturally, the fact that both PBLG and PCBL form helices of the same screw sense (right-handed) should favor such an induction effect, but it is rather surprising that the effect is still apparent even in sample

GLG-52 which contains as long a central CBL block as 60 residues.

The b_0 for a BLG-CBL diblock copolypeptide GL-6 is -405 at 20°C and decreases to -436 at 40°C. This fact indicates that the CBL block, which is partially helical even at 20°C, presumably due to conformational induction of the BLG block, becomes more helical at 40°C, and it is consistent with the observation that PCBL itself undergoes a thermally-induced coil-to-helix transition in the temperature range 20 - 40°C.[57,62-64]

Conformational induction has also been reported for DL and other types of block copolypeptides,[53,70,71] and the findings have been used to determine unknown screw senses of particular residues blocked with residues of known screw sense.[70,71] The degree of conformational induction is expected to depend on the sequence of the blocks as well as on the relative stability of their helices, i.e., the free energy difference between helical residues. Theories have been worked out in the conformations of various types of copolypeptides,[39,71,72] but they are not in the form amenable for a direct comparison with the present data. In this connection, we wish to remark that Klug and Applequist[71] have recently analyzed ORD data for a series of DL block copolypeptides

of varying DL ratios. They obtained a value of 100 - 400 cal/mol for the free energy difference between right- and left-handed α-helices of PBG and poly(L-tyrosine) compared it with an estimate from conformational analysis.[73] In the next chapter, we will develop a theoretical treatment of block copolypeptides and discuss their conformations statistical-mechanically.

3-5 Dielectric Dispersion

The dielectric method gives the dipole moment and relaxation time of the dissolved molecule, both of which are closely related to the molecular conformation. A polypeptide molecule in the helical conformation has a large electric dipole along the helix axis.[61,63, 74-85] The orientation of residue dipoles in the α-helix is schematically shown in Figure 3-4. For a rigid α-helical molecule, the resultant dipole moment may be proportional to the degree of polymerization. However, the dipole moment of a random coil or a broken-rod polypeptide may be different from that of the α-helical one, because the dipole moment is a vectorial quantity. Thus introduction of only one break in the helix is expected to bring about a drastic change in its dielectric characteristics. It is also pertinent to remark that the dielectric method is
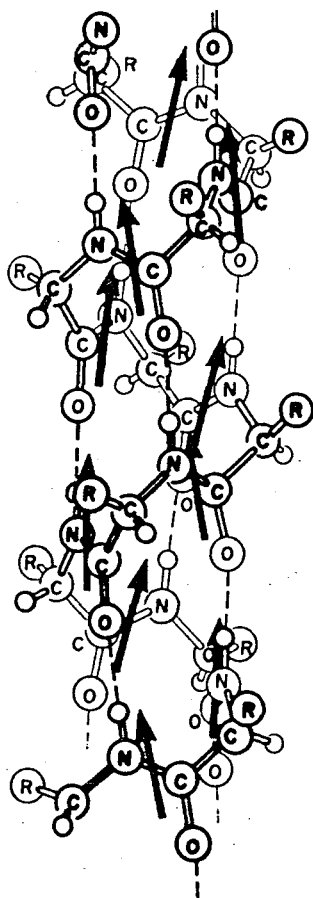
Figure 3-4.
Orientation of residue
dipole in the α-helix.[76]

particularly powerful for low molecular weight samples
studied here, to which the light-scattering method is not
always applicable with accuracy.

The dielectric dispersion of a solution characterized
by a single relaxation time τ obeys Debye's equations

$$\Delta\varepsilon' = \varepsilon_{\infty} + [\Delta\varepsilon/(1 + \omega^2\tau^2)] \qquad (3\text{-}2)$$

$$\Delta\varepsilon'' = \Delta\varepsilon\omega\tau/(1 + \omega^2\tau^2) \qquad\qquad (3\text{-}2)$$

where $\Delta\varepsilon'$ and $\Delta\varepsilon''$ are the real and imaginary parts of the complex dielectric constant of the solution in excess of those of the solvent, respectively. and $\Delta\varepsilon = \varepsilon_s - \varepsilon_\infty$, with ε_s being the static dielectric constant of the solution and ε_∞ the dielectric constant in the region of high frequency where only the solvent molecule contribute to the polarization. A plot of $\Delta\varepsilon''$ versus $\Delta\varepsilon'$, called the Cole-Cole plot, forms a semicircle with its center on the $\Delta\varepsilon'$ axis, and the segment cut out of the horizontal axis by the circle, i.e., the diameter of the circle, gives $\Delta\varepsilon$, and the frequency f_c corresponding to the summit of the arc is related to the mean rotational relaxation time τ by $\tau = 1/2\pi f_c$.

Figure 3-5 shows a typical Cole-Cole plots for samples GLG-331 and GL-6 in m-cresol at 20°C. The data points taken in the frequency range between 250 Hz and 2 MHz fall on a semicircle whose center is located near the $\Delta\varepsilon'$ axis. The closeness of the plot for GLG-331 to the Debye circle indicates that the sample is nearly homogeneous with respect to relaxation times, and hence with respect to molecular weights, too. Similar results were obtained for other fractionated samples. Since polydispersity may give
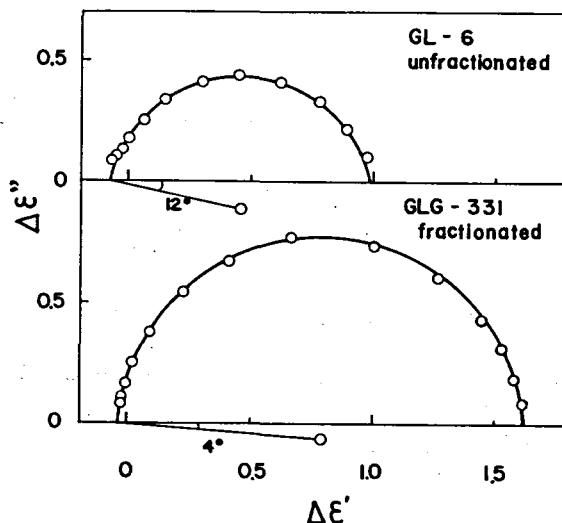
Figure 3-5.
Cole-Cole plots for samples GLG-331 and
GL-6 in m-cresol at 20°C.

rise to non-Debye type dispersions, the Cole-Cole plot may

be used as a sensitive measure of heterogeneity in

molecular weight. Looking at Figure 3-5, one sees that

unfractionated sample GL-6 gives a Cole-Cole plot whose

center is displaced a little more downward. This fact

suggests that this sample has a broader molecular weight

distribution than those of the fractionated samples.

However, from our previous studies with PBLG,[61] we infer

that the polydispersity index $\bar{M}_w/\bar{M}_n$ of sample GL-6 would

not have been more than 1.2, where $\bar{M}_n$ is the number-

average molecular weight.

In order to calculate the mean-square dipole moment from experimental vale for $\Delta\varepsilon$, we made use of the equation proposed by Applequist and Mahr,[79] which can be recast at the limit of infinit dilution in the form[61]

$$\langle\mu^2\rangle^{1/2} = (3kTM/4\pi N_A)(\Delta\varepsilon/c)(q/fg) \qquad (3\text{-}3)$$

where M is the molecular weight of the polypeptide, k is the Boltzmann constant, T is the absolute temperature, N_A is the Avogadro's number, and c is the solute concentration in g/ml. The factor q/fg depends primarily on the shape of the solute molecule; it is determined in particular by the axial ratio p for ellipsoids of revolution.[15,61,86] We here assume [15,61] that the molecular shape of a copolypeptide is approximated by an ellipsoid of revolution with an axial ratio equal to $\bar{N}_W/10$, with $\bar{N}_W$ being the weight-average degree of polymerization. Table 3-5, which summarizes the calculated results, shows that $\langle\mu^2\rangle^{1/2}$ for the triblock copolypeptides in m-cresol at $20^\circ C$ are approximately proportional to $\bar{N}_W$. This proportionality suggests that the molecular shape is rodlike, the fact compatible with the conclusion from the ORD data that the triblock copolypeptides examined are essentially helical under the same solvent conditions.

Table 3-5. Dielectric dispersion data for block
copolypeptides in m-cresol

Sample	$<\mu^2>^{1/2}$, D				$\tau T/\eta_0 \times 10^3$, sec deg/poise			
code	10°C	20°C	30°C	40°C	10°C	20°C	30°C	40°C
GLG-12	287	295	300	-	3.14	3.07	2.90	-
GLG-22	299	305	310	-	3.52	3.37	3.12	-
GLG-331	346	352	359	-	4.91	4.76	4.74	-
GLG-42	374	379	383	378	5.66	5.52	5.29	4.94
GLG-52	-	457	458	453	-	8.25	7.69	7.41
GL-6	227	234	-	-	2.89	2.79	-	-

If a triblock copolypeptide molecule assumes a
straight-rod shape in the temperature range investigated,
the resultant mean dipole moment may be expressed by the
following equation

$$\mu = \mu_G \bar{N}_G + \mu_L \bar{N}_L \qquad (3-4)$$

where μ_G and μ_L are the monomeric dipole moments in the
direction of the helix axis for BLG and CBL residues,
respectively, and $\bar{N}_G$ and $\bar{N}_L$ are the degree of
polymerization of BLG and CBL residues, respectively.
It is, however, reasonable to consider that some residues
at the ends of each block cannot be involved in a helical

section. Assuming that the number of such residues is constant and independent of the degree of polymerization, Eq. (3-4) is modified to

$$\mu - \mu_G \bar{N}_G = (\mu^* - \mu_G \bar{N}_G^* - \mu_L \bar{N}_L^*) + \mu_L \bar{N}_L \qquad (3\text{-}5)$$

where the asterisk denotes the values of a standard sample chosen arbitrarily. This equation predicts that a plot of $\mu - \mu_G \bar{N}_G$ versus $\bar{N}_L$ follows a straight line, that μ can be evaluated from the slope of the line, and that the ordinate intercept gives the contribution from the nonhelical loose ends. In Figure 3-6, the observed values
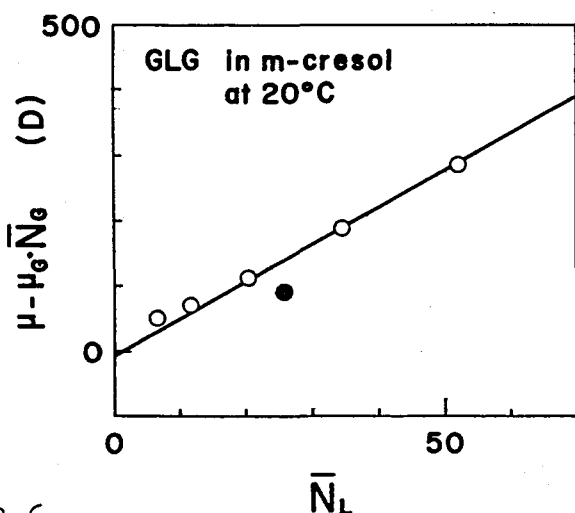
Figure 3-6.

A plot of $\mu - \mu_G \bar{N}_G$ versus the degree of polymerization $\bar{N}_L$ of CBL block. The value of 4.7 D was used for μ_G.[61] The full circle denotes the result for sample GL-6.

of $\mu - \mu_G \bar{N}_G$ are plotted against $\bar{N}_L$. Here we used for μ_G
the value of 4.7 (D) obtained by Matsumoto et al.[61] The
indicated line yields 5.6 $\pm$ 0.1 D for μ_L, which is in
fair agreement with 5.4 and 6.2 D deduced for PCBL in
m-cresol by Omura et al.[63] from dipole moment data in the
helix-coil transition region. Therefore we conclude that
the average dipole moment per residue is larger for CBL
than for BLG. Much lower values would be obtained for μ
if the central block were randomly coiled and bent. Note
that μ_G for once-broken rod PBLG is nearly half as large
as that for straight rod one.[61,78] In Figure 3-6, the
full circle denotes the result for sample GL-6. It
appears below the indicated line. This result means
incomplete helix formation of this sample, and is
consistent with the ORD data.

Figure 3-7 shows double-logarithmically the $\bar{N}_W$
dependence of mean rotational relaxation time τ corrected
for solvent viscosity η_0 and absolute temperature T. The
dashed lines denote the data by Matsumoto et al.[61] for
PBLG in helicogenic solvents. The data for the triblock
copolypeptides follow closely the curve for straight rod
PBLG and are much larger than those for once-broken rod
ones. These results also lend support to the conclusion
that the molecular shape of the triblock copolypeptides
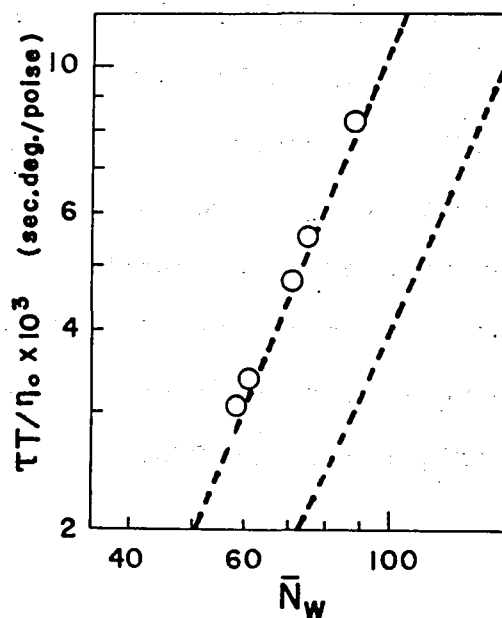
Figure 3-7.

Double logarithmic plot of $\tau T/\eta_0$ versus $\bar{N}_W$ for block copolypeptides of BLG and CBL in m-cresol at 20°C. The dashed lines denote the data for straight rog PBLG (upper) and for once-broken rod PBLG (lower), respectively.[61]

in m-cresol is essentially rodlike.

3-6 Intrinsic Viscosity

Intrinsic viscosities in a helix-breaking solvent DCA and in m-cresol are summarized in Table 3-6 and are compared in Figure 3-8, where the two dashed lines

represent the data for PBLG in DCA and in a helicogenic solvent DMF.[15,49] In this range of $\bar{N}_w$, the statistical radius of a polypeptide molecule should be smaller in the helical state than in the random coil state, and so is the intrinsic viscosity. The present data for the triblock copolypeptides are consistent with this prediction, because, as demonstrated by ORD and dielectric measurements, the molecular conformation is helical in m-cresol and randomly coiled in DCA.

Table 3-6. Viscosity data for block copolypeptides in DCA and m-cresol

Sample code	[η], dl/g		
	DCA 25°C	m-cresol 20°C	40°C
GLG-12	0.158	0.0785	0.0670
GLG-22	0.164	0.0840	0.0755
GLG-331	0.195	0.106	0.0970
GLG-42	0.198	0.112	0.103
GLG-52	0.220	0.115	0.107
GL-6	0.151	0.0895	0.0790
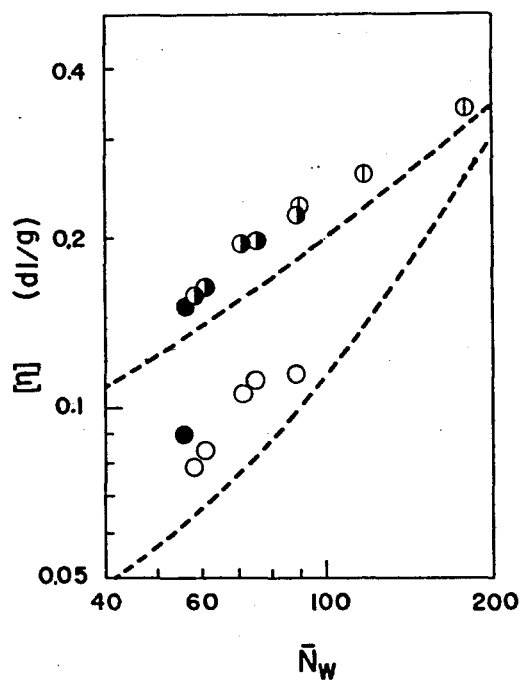
Figure 3-8.

Comparison of intrinsic viscosity - $\bar{N}_W$ relationships. (⬤), PCBL in m-cresol at 15°C, [57] (O), block copolypeptides in m-cresol at 20°C and (◕), in DCA at 25°C; (●), data for sample GL-6. The dashed lines denote the data for PBLG in DCA (upper) and in DMF (lower) at 25°C. [15,49]

3-7 Summary

Block copolypeptides of γ-benzyl L-glutamate and ε-carbobenzoxy L-lysine were synthesized by polymerization of the corresponding amino acid-N-carboxy anhydrides with initiation by n-butylamine. Optical rotatory dispersion data showed that the block copolypeptides of the type BLG-CBL-BLG were essentially helical in m-cresol at $20^{\circ}C$, despite the fact that in the same solvent conditions the isolated CBL chains assume completely random coiled conformation. Dielectric dispersion and viscosity data indicated the shape of the triblock copolypeptides was rodlike. These results suggest that the central CBL block is forced to take up a rigid helical conformation by an interaction from the flanking BLG blocks, which tend to assume a stable helical conformation under the solvent conditions studied. The conformational induction by the BLG blocks extend over a distance as long as 60 residues when each of the BLG blocks is 20 residues long.

Chapter 4

Helix-Coil Transition of Block Copolypeptides of

γ-Benzyl L-Glutamate and ε-Carbobenzoxy L-Lysine

4-1 Introduction

It has been shown in Chapter 3 that triblock

copolypeptides of the type BLG-CBL-BLG are essentially

helical in m-cresol at room teperature, although under the

same solvent condition, the isolated CBL chain of a length

similar to that of the central block is completely randomly

coiled. This fact is an example of the conformational

induction effect that have been demonstrated with various

combinations of peptide residues.[53,71,72] The extent of

conformational induction is expected to vary with the

solvent condition under which the polymer is studied as

well as with the residue combination. It is therefore

interesting to examine the conformation of the triblock

copolypeptide BLG-CBL-BLG in solvent mixtures of varying

helix-supporting power. In the work described below, we

have chosen mixtures of DCA and EDC for the reason that

detailed information was available about the helix-coil

transitions of the homopolypeptides of constituent

residues, PBLG and PCBL, in these mixtures.[30,32,56,57]

According to the well-established theories,[15,16] the

conformation of a helix-forming homopolypeptide in dilute solution is characterized by three parameters, i.e., the degree of polymerization of the polypeptide N, the equilibrium constant between helix and random coil residues s, and the helix-initiation parameter σ. Various attempts have been made to extend these theories to copolypeptides by introducing some additional assumptions and approximations.[12,13,33-40] However, their applications have been restricted only to random copolypeptides.[39,41-47] In this chapter, a similar theoretical approach aiming especially at block copolypeptides is presented. The derived theoretical expressions are used to predict characteristic features of the conformational induction in block copolypeptides and applied to detailed experimental data obtained for the BLG-CBL-BLG copolypeptides.

Our triblock copolymers exhibit an appreciable conformational transition at room temperature in DCA-EDC mixtures of such DCA contents in which PBLG is almost perfectly helical[30,56] but PCBL is randomly coiled.[32,57] Therefore, the homopolymer data for the transition parameters evaluated at different solvent compositions must be extrapolated to the solvent composition range appropriate for the copolymers. To check the validity of the extrapolation procedure employed, we have attempted a

direct determination of the transition parameters for PBLG
under the necessary solvent conditions and found a
satisfactory agreement between the direct and indirect
estimates.

4-2   Theoretical

The conformation of an α-helix-forming polypeptide in
solution can be described by the theory of Zimm and Bragg[17]
and of the subsequent authors.[18-22]   Here we follow Nagai's
formulation[22] in order to develop a theory adaptable to
block copolypeptides, especially of the type G-L-G.   The
theories of block copolypeptides proposed so far are not
necessarily in the form applicable to experimental data.[72]
At first, Nagai's theory[22] is described briefly, and its
extention to block copolypeptides is presented.

4-2-1   The Theory of Nagai for Homopolypeptides

Let us consider a homopolypeptide chain consisting of
N monomeric residues which are numbered 1, 2, ..., N from
the carboxy terminal.   For convenience of presentation, a
peptide residue ($-CO-HC^{\alpha}R-NH-$) is called helix unit when
distorted to the α-helical conformation, while it is random
coil unit when allowed to rotate around the bonds $C-C^{\alpha}$ and
$C^{\alpha}-N$.   Here R denotes the side chain attached to the

α-carbon. These units are designated h and c, respectively.
Thus a particular conformation of an α-helix-forming chain
is represented by sequence of the symbols h and c. The NH
group of the i-th residue is assumed to form a hydrogen
bond with the CO group of the (i+4)-th residue if and only
if the three residues between them are distorted
simultaneously to the α-helical conformation. To conform
to this α-helical conformation, therefore, it is necessary
to consider not only the nearest neighbor interaction but
also the interaction among essentially three consecutive
residues.

We now derive the partition function by the matrix
method, taking into account the interaction among four
consecutive residues. In so doing, we make use of a
transition probability matrix P whose elements are
determined by the statistical weights of the central
residue in three consecutive residues in seven different
conformations. The statistical weights assigned are as
follows:

$$
\begin{array}{ll}
\text{hhh} & s \\
\text{hch} & 1 \\
\text{chh} & \sigma^{1/2} \\
\text{cch} & 1 \\
\text{hhc} & \sigma^{1/2}
\end{array}
$$

hcc   1

ccc   1

We exclude two joint conformations chc and chhc, since these conformations, though not impossible, are physically unreasonable. This is because only one or only two consecutive distorted residues do not lead to the formation of intramolecular hydrogen bond. The parameter s is the statistical weight of a helix unit inside a helical sequence, or it may be interpreted as the equilibrium constant for the growing reaction of a helical sequence. The parameter $\sigma^{1/2}$ is the statistical weight of the terminal unit of a helical sequence and called the cooperativity parameter for the formation of helical sequences.

   If it is assumed that the carboxyl group and amino group of the terminal residues of the chain are not capable of hydrogen-bonding, the partition function of an α-helix-forming chain consisting of N residues, Z_N, can be written

$$Z_N = \underset{\sim}{e}_1 \underset{\sim}{P}^{N-2} \underset{\sim}{e}_N \qquad\qquad (4-1)$$

with the transition probability matrix $\underset{\sim}{P}$ give by

| i-2 | i-1 | i | i+1 | h | h | h | h | c | c | c |
| | | | i | h | c | h | c | h | c | c |
			i-1	h	h	c	c	h	h	c
h	h	h	$P =$	s	0	0	0	$\sigma^{1/2}$	0	0
h	c	h		0	0	$\sigma^{1/2}$	0	0	0	0
c	h	h		s	0	0	0	0	0	0
c	c	h		0	0	$\sigma^{1/2}$	0	0	0	0
h	h	c		0	1	0	0	0	1	0
h	c	c		0	0	0	1	0	0	1
c	c	c		0	0	0	1	0	0	1

$$(4\text{-}2)$$

Since the first and N-th residues cannot be involved in a helical section, the end vectors associated with the first and N-th residues are written

$$e_1 = (0,\ 0,\ 0,\ 1,\ 0,\ 0,\ 1)$$

$$e_N = (0,\ 0,\ 0,\ 0,\ 1,\ 1,\ 1)^T \qquad (4\text{-}3)$$

respectively, where the superscript T denotes the transpose of a vector.

The characteristic equation of P is found to be

$$\lambda^2(\lambda - s)(\lambda - 1) = s\sigma \qquad (4\text{-}4)$$

The eigenvalues of P, i.e., the root of this equation, are

denoted by λ_1, λ_2, λ_3, and λ_4 in their order of magnitude, i.e., $\lambda_1 > .. > \lambda_4$. With these eigenvalues, the right- and left-hand eigenvectors, $\underset{\sim}{U}(\lambda)$ and $\underset{\sim}{V}(\lambda)$, are expressed as

$$\underset{\sim}{U}(\lambda) = (1, \frac{s\sigma^{1/2}}{\lambda^2}, \frac{s}{\lambda}, \frac{s\sigma^{1/2}}{\lambda^2}, \frac{\lambda-s}{\sigma^{1/2}}, \frac{\lambda-s}{\sigma^{1/2}}, \frac{\lambda-s}{\sigma^{1/2}})^T$$

$$\underset{\sim}{V}(\lambda) = c(\lambda)(1, \frac{\sigma^{1/2}}{\lambda^2}, \frac{\lambda-s}{s}, \frac{\lambda-s}{s\sigma^{1/2}}, \frac{\sigma^{1/2}}{\lambda}, \frac{\sigma^{1/2}}{\lambda^2}, \frac{\lambda-s}{s\sigma^{1/2}})$$

$$(4-5)$$

where

$$c(\lambda) = \lambda(\lambda - 1)F(\lambda)$$

with

$$F(\lambda) = 1/[4\lambda^2 - 3(1 + s)\lambda + 2s]$$

Since the matrices $\underset{\sim}{P}$ and $\underset{\sim}{P}^{N-2}$ may be expanded as

$$\underset{\sim}{P} = \sum_{i=1}^{4} \lambda_i \underset{\sim}{U}(\lambda_i)\underset{\sim}{V}(\lambda_i) \tag{4-6}$$

$$\underset{\sim}{P}^{N-2} = \sum_{i=1}^{4} \lambda_i^{N-2} \underset{\sim}{U}(\lambda_i)\underset{\sim}{V}(\lambda_i) \tag{4-7}$$

Eq. (4-1) is brought to the expression

$$Z_N = \sum_{i=1}^{4} \lambda_i^{N-2}[\underset{\sim}{e}_1 \underset{\sim}{U}(\lambda_i)\underset{\sim}{V}(\lambda_i)\underset{\sim}{e}_N]$$

$$= \sum_{i=1}^{4} \lambda_i^{N}(\lambda_i - s)F(\lambda_i) \tag{4-8}$$

By using Z_N thus obtained Nagai has derived expressions for

-49-

various important average quantities which characterize the equilibrium conformation of α-helix-forming polypeptide chain.[22] Two of them are given below.

The average fraction of intact hydrogen bonds in the chain, Θ_N, is represented by

$$\Theta_N = N^{-1}\partial(\ln Z_N)/\partial(\ln s) \qquad (4\text{-}9)$$

Substitution of Eq. (4-8) yields

$$\Theta_N = N^{-1}Z_N^{-1}\sum_{i=1}^{4}\lambda_i^{N}[Nc(\lambda_i)\zeta(\lambda_i) - I_1(\lambda_i)] \qquad (4\text{-}10)$$

where

$$\zeta(\lambda) = (\lambda - s)F(\lambda)$$
$$I_1(\lambda) = 2\lambda(\lambda - 1)(\lambda - s)(2\lambda^2 - s)F(\lambda)^3$$

The average fraction of helix units in the chain, f_N, can be calculated from

$$f_N = N^{-1}[\partial(\ln Z_N)/\partial(\ln s) + \partial(\ln Z_N)/\partial(\ln \sigma^{1/2})]$$

$$= N^{-1}Z_N^{-1}\sum_{i=1}^{4}\lambda_i^{N}[Nf(\lambda_i)\zeta(\lambda_i) - I_2(\lambda_i)] \qquad (4\text{-}11)$$

where

$$f(\lambda) = (\lambda - 1)(3\lambda - 2s)F(\lambda)$$
$$I_2(\lambda) = 2\lambda(\lambda - 1)(\lambda - s)(6\lambda^2 - 8s\lambda + 3s^2)F(\lambda)^3$$

4-2-2 Theory of Triblock Copolypeptides

We next develop a proper form of the partition function for a triblock copolypeptide of the type G-L-G; G and L denote two kinds of amino acid residues. As in the case of homopolypeptide discussed above, it is assumed that the statistical weight of a central residue in given three consecutive residues is determined by the joint conformation of the three residues concerned, but this time their residue arrangement has to be taken into account. Then each residue, excepting those located at G-L and L-G block boundaries, may be given the transition probability matrix characteristic of the corresponding homopolypeptide. At least four residues at a block boundary need a separate consideration, because each of them lies in a different residue arrangement from each other. However, we here assume that each residue is given the transition probability matrix characteristic of the corresponding homopolypeptide irrespective of its location. This assumption is equivalent to replacing the statistical weights of the boundary residues by the geometric means of the corresponding ones of the two residues G and L. Effect of such a replacement on average quantities of the molecule may be relatively small, the population of the boundary residues being small in the block copolypeptides

to be considered. The validity of this approximate treatment, however, has to be tested with experimental data.

Let us consider a triblock copolypeptide $(BLG)_m$-$(CBL)_n$-$(BLG)_p$ having m,n,and p residues on each block. Application of Nagai's theory[22] to this polypeptide, with the assumption introduced above, gives the partition function Z_N of the form:

$$Z_N = \underset{\sim}{e}_1 (\underset{\sim}{P}_G)^{m-1} (\underset{\sim}{P}_L)^n (\underset{\sim}{P}_G)^{p-1} \underset{\sim}{e}_N \qquad (4\text{-}12)$$

where the subscripts G and L refer to BLG and CBL, respectively, and N = m + n + p. After similar manipulations employed in the previous section, Eq. (4-12) is transformed to

$$Z_N = \underset{\sim}{e}_1 [\sum_{i=1}^{4} \lambda_{Gi}^{m-1} \underset{\sim}{U}(\lambda_{Gi}) \underset{\sim}{V}(\lambda_{Gi})] [\sum_{j=1}^{4} \lambda_{Lj}^{n} \underset{\sim}{U}(\lambda_{Lj}) \underset{\sim}{V}(\lambda_{Lj})]$$

$$\times [\sum_{k=1}^{4} \lambda_{Gk}^{p-1} \underset{\sim}{U}(\lambda_{Gk}) \underset{\sim}{V}(\lambda_{Gk})] \underset{\sim}{e}_N$$

$$= \sum_{i,j,k=1}^{4} \lambda_{Gi}^{m-1} \lambda_{Lj}^{n} \lambda_{Gk}^{p-1} \underset{\sim}{V}(\lambda_{Gi}) \underset{\sim}{U}(\lambda_{Lj}) \underset{\sim}{V}(\lambda_{Lj}) \underset{\sim}{U}(\lambda_{Gk})$$

$$\times [\underset{\sim}{e}_1 \underset{\sim}{U}(\lambda_{Gi}) \underset{\sim}{V}(\lambda_{Gk}) \underset{\sim}{e}_N]$$

$$= \sum_{i,j,k=1}^{4} \lambda_{Gi}^{m} \lambda_{Lj}^{n} \lambda_{Gk}^{p} V(\lambda_{Gi}) U(\lambda_{Lj}) V(\lambda_{Lj}) U(\lambda_{Gk})$$

$$= \sum_{i,j,k=1}^{4} \lambda_{Gi}{}^{m} \lambda_{Lj}{}^{n} \lambda_{Gk}{}^{p} \underset{\sim}{V}(\lambda_{Gi}) \underset{\sim}{U}(\lambda_{Lj}) \underset{\sim}{V}(\lambda_{Lj}) \underset{\sim}{U}(\lambda_{Gk})$$

$$\times \ (\lambda_{Gi} - s_G) F(\lambda_{Gk}) \qquad (4\text{-}13)$$

where λ_{Gi} and λ_{Lj} (i,j=1, 2, 3, 4) are the roots of
Eq. (4-4), with s and σ being replaced by s_G and σ_G and s_L
and σ_L, respectively. The helical fraction of block
copolypeptide can be calculated by Eq. (4-9) with

$$\partial/\partial(\ln s) = \partial/\partial(\ln s_G) + \partial/\partial(\ln s_L) \qquad (4\text{-}14)$$

4-2-3 Theoretical Predictions

It has been shown in Chapter 3 that the central CBL
block in a triblock copolypeptide of the type BLG-CBL-BLG
is forced to take up an α-helical conformation in m-cresol
in which PCBL itself undergoes a sharp thermal transition.
At first, we shall explain this conformational induction
by using the copolymer theory developed in the previous
section. PBLG is known to form a stable α-helix in
m-cresol with the transition parameters of s_G = 1.61 and
$\sigma_G{}^{1/2}$ = 0.04,[60] while the thermal transition of PCBL in
m-cresol is characterized by a much smaller $\sigma_L{}^{1/2}$ of
0.0025.[57] In the discussion to follow, these parameter
values are used to test theoretical predictions on the
helix stability of the triblock copolypeptide under the

solvent conditions considered.

Figure 4-1 illustrates the dependence of helical fraction Θ_N on the degree of polymerization N_L of the central CBL block as a function of s_L, with the degree of polymerization N_G of each flanking BLG block being fixed at 20. It is seen that Θ_N first increases, passes through a maximum, and then decreases gradually with increasing N_L.
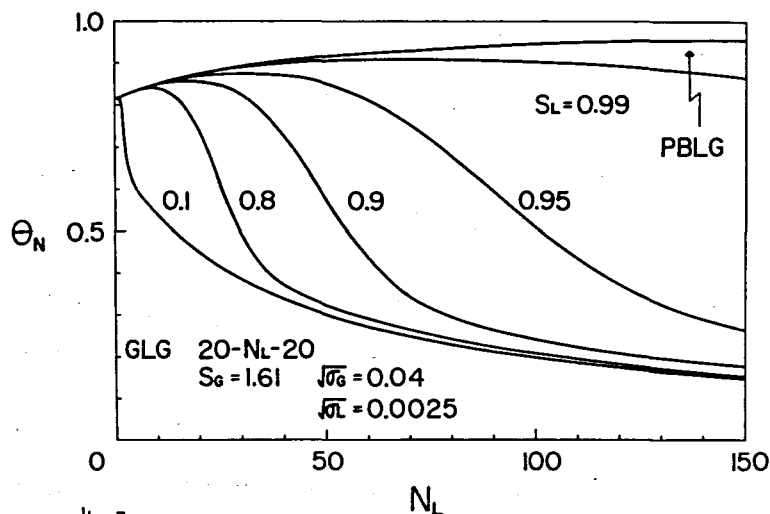
Figure 4-1.
Plots of helical fraction Θ_N versus the degree of polymerization N_L of central CBL block as a function of s_L, with the degree of polymerization N_G of each flanking BLG block being fixed at 20; 20-N_L-20. The curve labeled as PBLG indicates the theoretical values of Θ_N for PBLG having the same degree of polymerization as the triblock copolypeptide. The parameters chosen are $s_G=1.61$, $\sigma_G^{1/2}=0.04$, and $\sigma_L^{1/2}=0.0025$.

However, for $s_L > 0.95$, the change in θ_N with N_L is very small at least up to N_L of 60. The values of θ_N are converted to the average number of helical residues N_h and plotted against N_L in Figure 4-2. Unless s_L is too small, N_h first increases linearly with N_L, which implies that a short CBL block sandwiched between BLG blocks is always forced to assume helical conformation. Near the transition point for the CBL block, i.e., for s_L close to unity, N_h tends to increase steadily with N_L. As N_L is increased further, N_h tends to decrease toward some asymptotic value
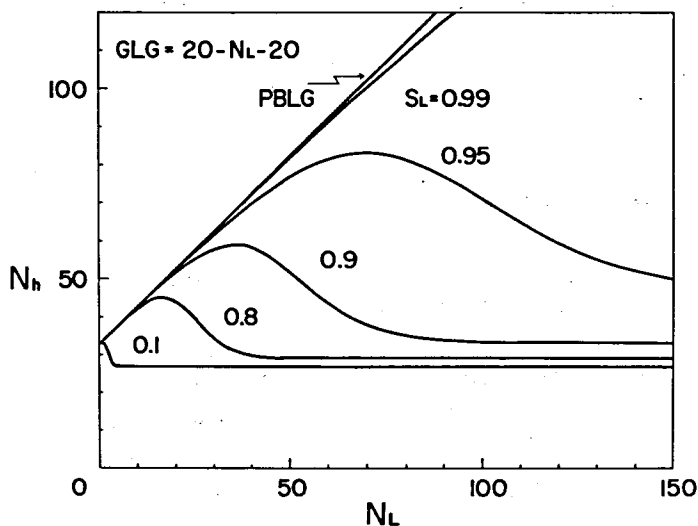
Figure 4-2.
Plots of the average number of helical residues N_h versus N_L as a function of s_L, with N_G being fixed at 20.
The same parameters as those in Figure 4-1 are used.

depending on s_L. Panel(a) of Figure 4-3 shows how Θ_N varies with N_G for a fixed N_L of 40 and a set of the transition parameters: $s_G = 1.61$, $\sigma_G^{1/2} = 0.04$, $s_L = 0.99$, and $\sigma_L^{1/2} = 0.0025$. It is to be noted that N_G of 8 is large enough to bring about an appreciable conformational induction for the parameter values chosen. Panel(b) of the same figure indicates that inequality of the chain lengths of the two flanking blocks has little effect on Θ_N if they are longer than 8. This critical length of BLG chain may be compared with the previous estimate of the
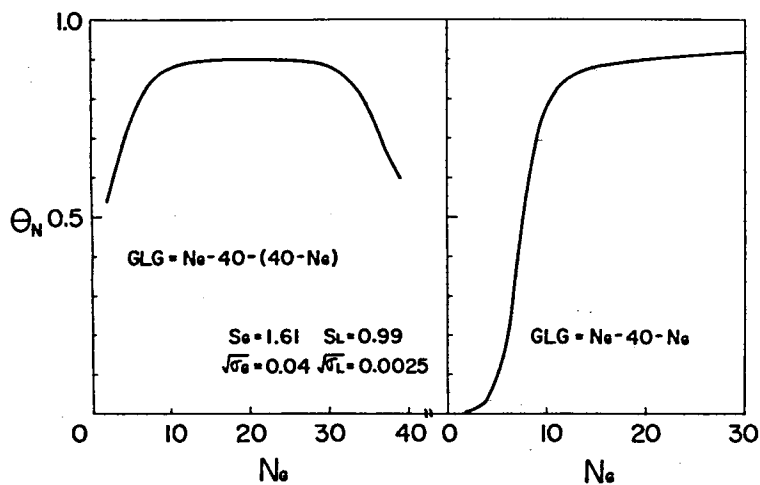
Figure 4-3.   (b)   (a)
Plots of Θ_N versus N_G, with N_L being fixed at 40. The parameters chosen are $s_G = 1.61$, $\sigma_G^{1/2} = 0.04$, $s_L = 0.99$, and $\sigma_L^{1/2} = 0.0025$.

minimum chain length required for the formation of an

α-helix, which is between 6 and 10.[53,71]

Figure 4-4 demonstrates the s_L dependence of Θ_N as a

function of s_G for a triblock copolypeptide 20 - 40 - 20,

when $\sigma_G^{1/2}$ = 0.04 and $\sigma_L^{1/2}$ = 0.0025. The conformational

induction is seen to occur adruptly at some s_L value, which

become larger for smaller s_G. Even for s_G < 1.0, Θ_N

becomes greater than 0.5 for larger s_L; only if all the

CBL residues were in the helical conformation, Θ_N would be

0.5. This implies that helix formation is promoted by the
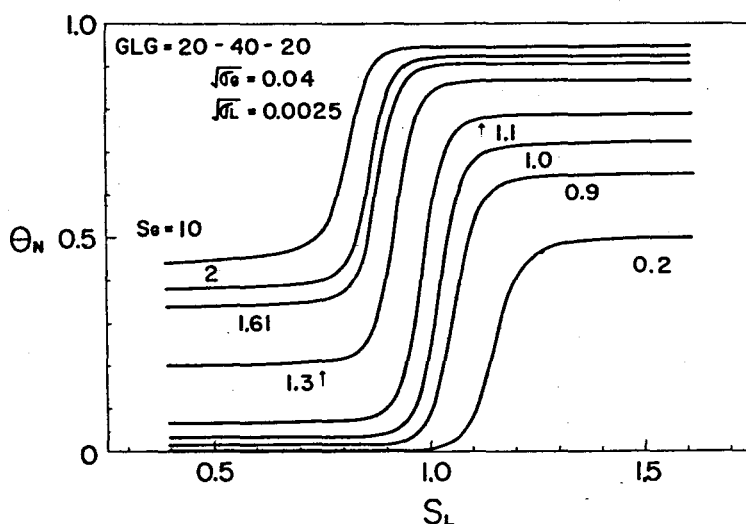
Figure 4-4.
The s_L dependence of Θ_N as a function of s_G for a
triblock copolypeptide 20-40-20, when $\sigma_G^{1/2}$ = 0.04 and
$\sigma_L^{1/2}$ =0.0025.

central CBL block as its helix stability becomes greater
than that of the BLG blocks.

In Figure 4-5 are plotted the values of Θ_N against s_G,
with s_L as parameter. The change in Θ_N with s_G is more
gradual than that with s_L depicted in Figure 4-4. This
fact predicts that s_G is the main determining factor for
the helix stability of the triblock copolypeptide. The
experimental finding that the conformational induction by
the BLG blocks extends over 60 CBL residues is consistent
with the theoretical arguments presented above, because
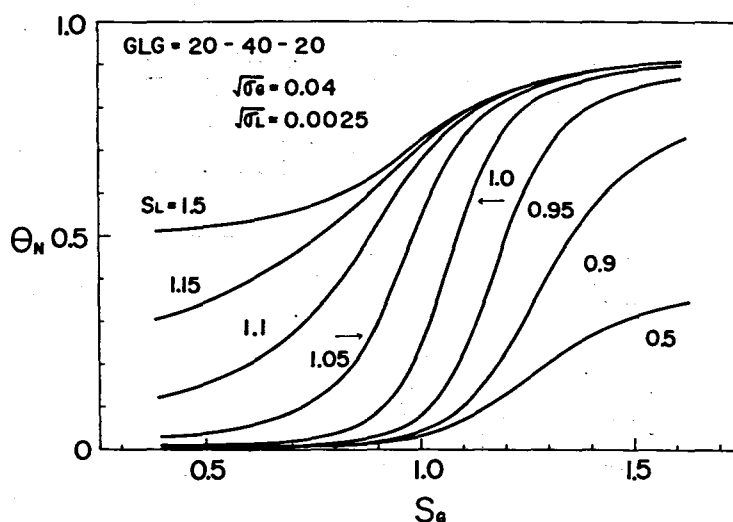
Figure 4-5.
The s_G dependence of Θ_N as a function of s_L for a
triblock copolypeptide, when $\sigma_G^{1/2}=0.04$ and $\sigma_L^{1/2}=0.0025$.

the s_L value in m-cresol is estimated to be about 1.000 $\pm$ 0.004[57] and because N_G is larger than 10 for all of the samples studied.

4-3 Experimental Results

Five samples of G-L-G triblock copolypeptide, one G-L block copolypeptide sample, and five PBLG sample were subjected to ORD measurements, with DCAOEDC mixtures as solvent. Their molecular weights and compositions are given in Table 4-1.

Figure 4-6 shows the thermal transition curves of sample GLG-331 in DCA-EDC mixtures of indicated volume ratios. One can observe that the triblock copolypeptide undergoes a thermally-induced coil-to-helix transition of inverse type, and that the transition behavior depends remarkably on solvent composition. The transition appears to become sharpest between 50 and 55 vol-% DCA, and this composition range may be compared with about 75 vol-% for PBLG[30,56] and 33 vol-% for PCBL.[32,57] It is interesting to note that an alternating copolypeptide of BLG and CBL, poly(ϵ-carbobenzoxy-L-lysyl-γ-benzyl-L-glutamate), undergoes an inverse thermal transition in a similar composition range.[87,88]

Table 4-1.   Degrees of polymerization of block
copolypeptides and PBLG

Sample code	$\bar{M}_w \times 10^{-4}$	$\bar{N}_w$	$\bar{N}_G$	$\bar{N}_L$
GLG-12	1.31	58.5	51.9	6.6
GLG-22	1.39	61.1	49.6	11.5
GLG-331	1.64	71.0	50.8	20.2
GLG-42	1.79	74.9	40.5	34.4
GLG-52	2.16	88.5	36.4	52.1
GL-6	1.34	56.1	30.4	25.7
A-2	0.476	21.8		
A_n-4[a]	0.85[b]	39		
A-3	1.06	48.4		
A-43	1.46	66.7		
A_n-22	3.38	154		
E-2	23.7			

a.   PBDG sample.

b.   Viscosity-average molecular weight.
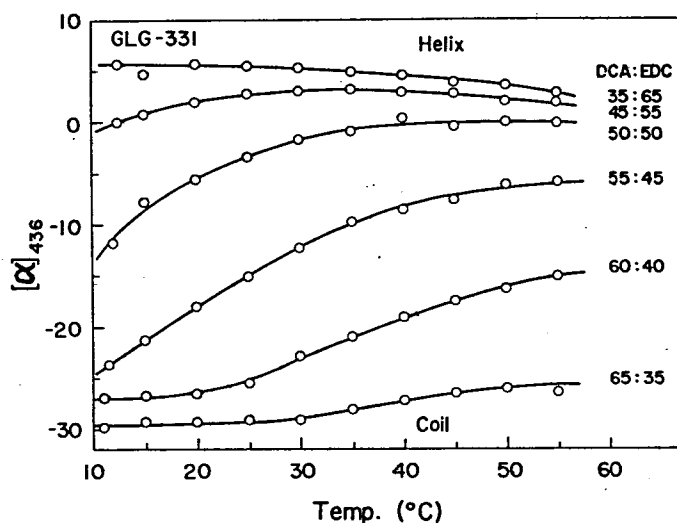
Figure 4-6.
Temperature dependence of specific rotation at 436 nm,
$[\alpha]_{436}$, for sample GLG-331 in DCA-EDC mixtures of
different compositions. Compositions are indicated by
volume ratios of DCA to EDC at 25°C.

Figure 4-7 shows the transition curves of PBLG in a

DCA-EDC mixture (55 vol-% DCA) as functions of molecular

weight, where the data for GLG-331 are replotted for

comparison. The transition curve of GLG-331 lies far

below that of PBLG sample of the same chain length but

above that expected for an isolated flanking BLG block
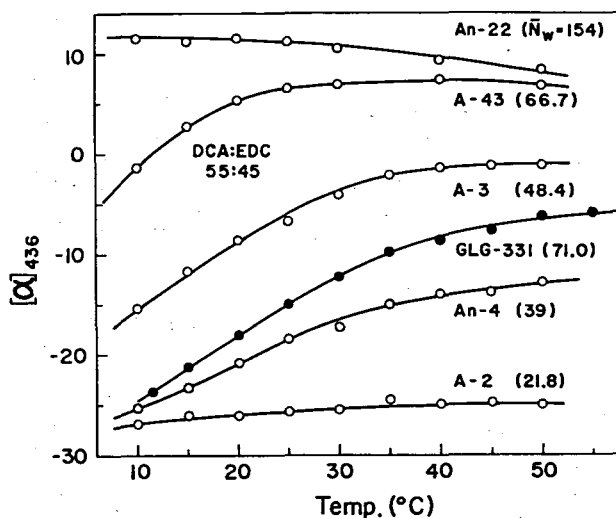
Figure 4-7.

Temperature dependence of $[\alpha]_{436}$ for GLG-331 and PBLG in a DCA-EDC mixture (55 vol-% DCA) as a function of weight-average degree of polymerization $\bar{N}_W$. The value of $[\alpha]_{436}$ for sample PBDG A_n-4 are indicated by changing their signs.

($\bar{N}_W \approx 25$). This finding may also be taken as evidence for

the conformational induction that has occurred in the

DCA-EDC mixture studied.

4-4 Analysis of Transition Curves

4-4-1 PBLG Data

At first, ORD data for PBLG in a DCA-EDC mixture (55 vol-% DCA) as functions of molecular weight are analyzed to evaluate the transition parameters s_G and σ_G. As is usually done, the helical fraction is calculated from the Moffitt parameter b_0 by

$$\text{helical fraction} = (b_0 - b_0^C)/(b_0^H - b_0^C) \qquad (4\text{-}15)$$

where b_0^H and b_0^C denote the values of b_0 for perfect helix and random coil, respectively. Theoretical calculations with helical polypeptides have suggested that b_0 is more closely related to the number of intact hydrogen bonds than to the number of helical residues.[89,90] Therefore, we here regard the quantity on the right-hand side of Eq. (4-15) as θ_N rather than f_N. No such differentiation is necessary in usual cases where larger molecular weights are treated.[16]

The use of Eq. (4-15) for evaluating θ_N faces a difficult problem of how to determine the values of b_0^H and b_0^C, because these quantities usually depend on polypeptide-solvent systems chosen,[57] and in some cases, also on temperature.[32,60,91,92] To solve this problem, ORD data

were taken on three PBLG samples of different molecular
weights (A-2, A_n-4, E-2) in DCA-EDC mixtures (20 and 90
vol-% DCA) over the temperature range 10 - 50°C. The
values of b_0 in the 90 vol-% DCA were found to vary little
with temperature and molecular weight, and hence their
average was taken as b_0^C. On the other hand, the b_0 value
in the 20 vol-% mixture, which is considered to be
strongly helix supporting, changed from -630 to -610 as
the temperature was increased from 10 to 50°C. Thus, the
value at each temperature was taken as b_0^H at that
temperature.

Data for Θ_N at a given temperature were fitted to
Nagai's theoretical expression, Eq. (4-10),[22] to evaluate
the values of s and $\sigma^{1/2}$ at that temperature. The curve
fitting operation was truncated when the quantity τ
defined by

$$\tau = \sum_i [(\Theta_{N,expt})_i - (\Theta_{N,calcd})_i]^2 \qquad (4\text{-}16)$$

become minimum, where the summation was carried out over
all the possible samples examined, with $\Theta_{N,expt}$ and
$\Theta_{N,calcd}$ being the experimental values of Θ_N and
theoretical ones calculated for the corresponding N and
a given set of s and $\sigma^{1/2}$, respectively. Figure 4-8
illustrates the curve-fitting procedure with the data for
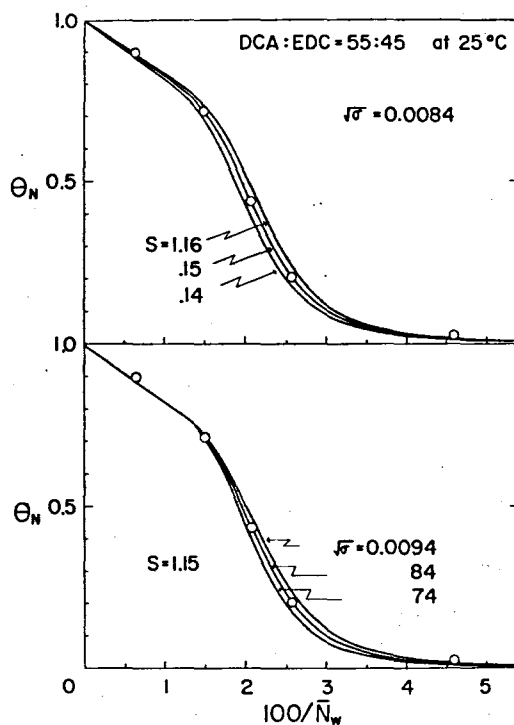
Figure 4-8.
Dependence of Θ_N on the degree of polymerization for
PBLG in a DCA-EDC mixture (55 vol-% DCA) at 25°C.
The circles are the experimental values for Θ_N, which
are estimated from b_0 by using Eq. (4-15), and the
solid lines represent the theoretical ones calculated
for the indicated parameter values.

a DCA-EDC mixture (55 vol-% DCA) at $25^{\circ}C$, where the solid

lines indicate the theoretical Θ_N calculated by using

Eq. (4-10) for the sets of values s and $\sigma^{1/2}$ indicated

and the circles denote the experimental Θ_N values. It is

seen that there exists a range of s and $\sigma^{1/2}$ which fit

the theory equally well to experimental points.

Therefore, their central values were taken as those for

the solvent condition chosen. Similar procedures were
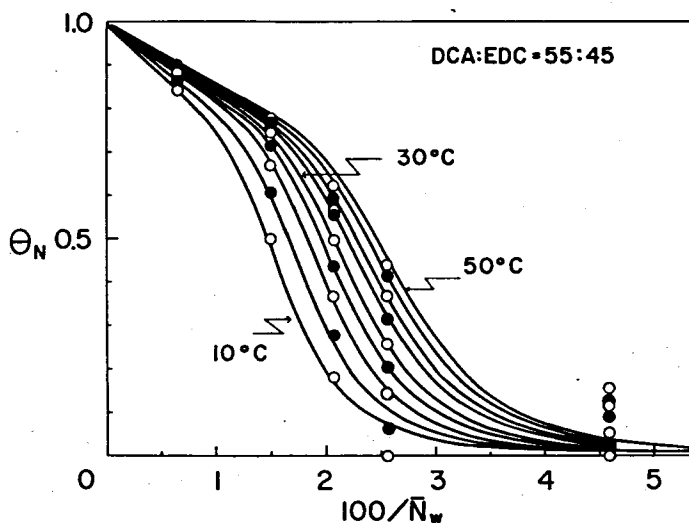
Figure 4-9.
Plots of Θ_N versus $1/\bar{N}_W$ for PBLG in a DCA-EDC mixture
(55 vol-% DCA) at 50, 45, 40, 35, 30, 25, 20, 15, and
$10^{\circ}C$ from top to bottom. The solid lines represent
the theoretical values calculated for the respective
sets of values s_G and $\sigma_G^{1/2}$ given in Table 4-2.

Table 4-2. Transition parameters of PBLG in a
mixture of DCA-EDC (55 vol-% DCA)

Temp. °C	s_G	$\sigma_G^{1/2} \times 10^2$	$s_{G,calcd}$[a]
10	1.10	0.75	1.13
15	1.12	0.76	1.15
20	1.14	0.76	1.16
25	1.15	0.84	1.17
30	1.16	0.89	1.18
35	1.17	0.98	1.18
40	1.18	1.00	1.19
45	1.19	1.04	1.19
50	1.20	1.06	1.19

a. Calculated values from the data
   of Sayama et al.[30]

applied to the data at other temperature. The resulting
s and $\sigma^{1/2}$ as a function of temperature are summarized in
Table 4-2. Figure 4-9 shows plots of Θ_N versus $1/\bar{N}_W$ in
the same DCA-EDC mixture at various temperatures. The
solid lines represent the theoretical values calculated
with the values of s and $\sigma^{1/2}$ given in Table 4-2. The

agreement between theory and experiment is satisfactory
except for the lowest-molecular-weight sample.

4-4-2   Block Copolypeptide Data

Determination of helical fraction for block
copolypeptides may also be carried out by using Eq. (4-15),
but this time b_0^H and b_0^C may depend on polypeptide
composition.   The b_0 values contain contributions from BLG
as well as CBL blocks and may be expressed as

$$b_0 = X(b_0)_L^\xi + (1 - X)(b_0)_G^\xi \qquad (\xi = H \text{ or } C) \qquad (4-17)$$

where X denotes the mole fraction of CBL residues, and
$(b_0)_G^\xi$ and $(b_0)_L^\xi$ represent the values of b_0 of PBLG and PCBL,
respectively.   The available data[32] for $(b_0)_G^\xi$ and $(b_0)_L^\xi$
were substituted into Eq. (4-15) to determine the helical
fraction of each sample at desired temperature.

Figure 4-10 shows the temperature dependence of b_0
for block copolypeptides consisting of BLG and CBL blocks
in a DCA-EDC mixture (55 vol-% DCA).   The transition curve
shifts toward higher temperature and becomes gradual as
the CBL content in the sample is increased.   These b_0 data
are converted to Θ_N by the procedure described above and
analyzed by the theory developed in Sction 4-2.   The
theory gives Θ_N as a function of s_G, σ_G, s_L, σ_L, N_G, and
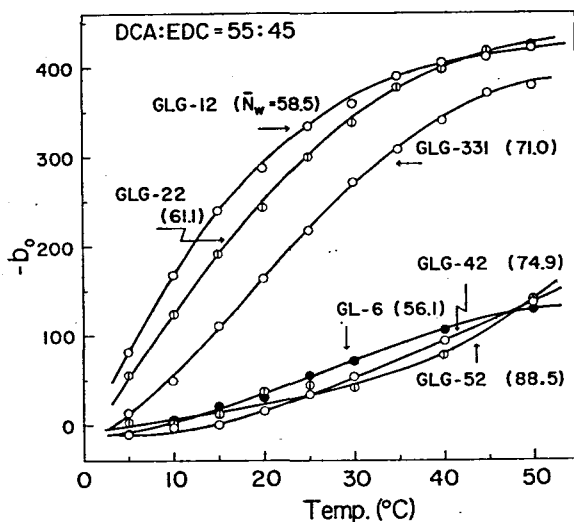
Figure 4-10.
Temperature dependence of Moffitt parameter b_0 for block copolypeptides in a DCA-EDC mixture (55 vol-% DCA).

and N_L. We may use the values of N_G and N_L given in Table 4-1 and the data for s_G and σ_G determined in the previous section (Table 4-2). Since σ is essentially independent of solvent composition and temperature,[30-32] we may take $\sigma_L^{1/2}$ to be 0.003, the average value of $\sigma^{1/2}$ obtained previously for PCBL in DCA-EDC mixtures of lower DCA contents.[32] With these parameter values, Θ_N were calculated for each sample and selected temperatures as a function of s_L, and the value of s_L which gave the best

Table 4-3. Transition parameters of PCBL in a
DCA-EDC mixture (55 vol-% DCA) at
various temperatures

Temp. $^{\circ}$C	s_L $(\sigma_L^{1/2}=0.003)$					$s_{L,calcd}$ [a]
	GLG-12	GLG-22	GLG-331	GLG-42	GLG-52	
5	0.96	0.95	0.81	–	–	0.76
10	1.04	0.99	0.92	–	–	0.78
15	1.04	1.00	0.95	–	0.81	0.80
20	1.01	0.99	0.95	0.86	0.97	0.82
25	1.01	1.00	0.95	0.92	0.96	0.83
30	1.03	1.00	0.95	0.93	0.96	0.85
35	1.00	1.01	0.95	–	–	0.86
40	0.99	1.01	0.95	0.94	0.97	0.87
45	0.95	1.02	0.95	–	–	0.88
50	0.93	1.00	0.94	0.94	0.97	0.89

a. Calculated values from the data of Maekawa et al.[32]

agreement between theory and experiment was chosen. The
values of s_L thus chosen are summarized in Table 4-3.
Although these values of s_L scatter between 0.8 and 1.04
depending on temperature and sample, a value of 0.95 may
be taken as their average.
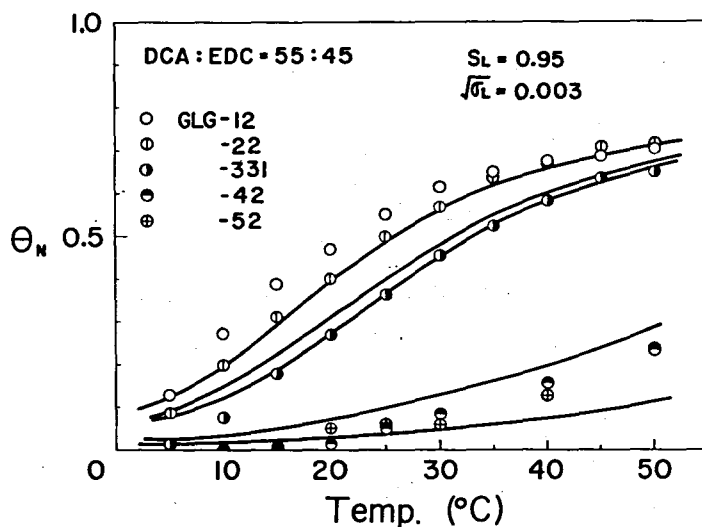
Figure 4-11.
Comparison between theoretical values and experimental
ones, where the solid lines represent the theoretical
Θ_N computed for $s_L = 0.95$ and the circles denote the
experimental values. The data for s_G and $\sigma_G^{1/2}$ listed
in Table 4-2 and $\sigma_L^{1/2} = 0.003$ were used to estimate the
theoretical values.

In Figure 4-11, the solid lines represent the
theoretical Θ_N computed for $s_L = 0.95$ and the circles
denote the experimental values. Agreement between theory
and experiment is not necessarily satisfactory. For an
illustrative purpose, the theoretical curves of sample
GLG-331 for various sets of s and $\sigma^{1/2}$ are shown in
Figure 4-12. The top panel examines the effect of s_L on
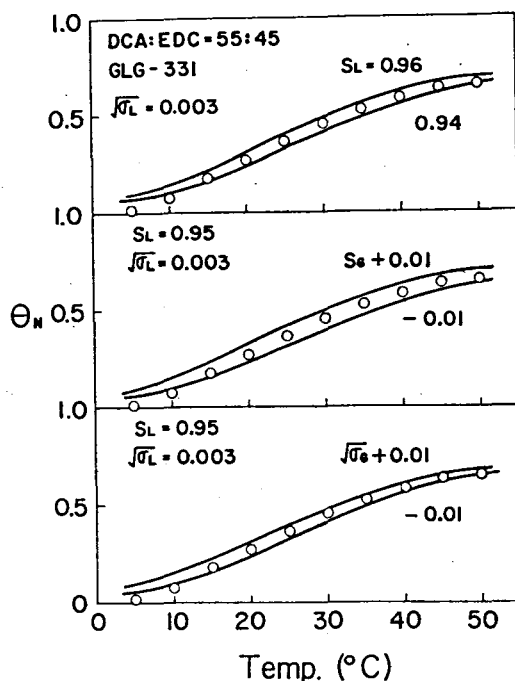
Figure 4-12.
Comparison between theoretical values and experimental ones, where the solid lines represent the theoretical Θ_N and the circles denote the experimental values; s_L is varied in the top panel, while s_G and $\sigma_G^{1/2}$ are varied in the middle and bottom panels, respectively. The same parameters as those in Figure 4-11 are used for the computations.

Θ_N, whereas the middle and bottom panels show the effects of s_G and σ_G, respectively. It can be seen that Θ_N is more sensitive to s_G and σ_G than to s_L. It was found that $\sigma_L^{1/2}$ had little effect on the calculated Θ_N. This

-72-

calculation suggests that the helical stability of flanking BLG blocks plays a more decisive role than that of the central block in determining the conformation of the entire molecule, at least, in our special case where PBLG helix is more stable than PCBL helix in the given solvent condition.

4-5   Discussion

For a solvent mixture composed of a non-polar liquid such as EDC and an organic acid such as DCA, the equilibrium constant s depends both on temperature T and the activity a of the acid component. It has been shown that [29,30]

$$s = s_0/(1 + Ka) \qquad\qquad (4\text{-}18)$$

where s_0 is the value of s in the non-polar solvent and K is the equilibrium constant between peptide residue and dimeric acid. K and s_0 are function only of T and may be expressed as [30]

$$s_0 = \exp[-(\Delta H_0 - T\Delta S_0)/RT] \qquad\qquad (4\text{-}19)$$

$$K = \exp[-(\Delta H_a - T\Delta S_a)/RT] \qquad\qquad (4\text{-}20)$$

where R is the gas constant and ΔH_0, ΔS_0, ΔH_a, and ΔS_a

are the parameters independent of T. Equation (4-18)
combined with Eqs. (4-19) and (4-20) allows s to be
determined as a function of T and a, provided that the
values of these parameters are available. The relevant
data for PBLG[30] and PCBL[32] in DCA-EDC mixtures found in
the literature are reproduced in Table 4-4. With these
data , we have calculated the values of s_G and s_L in a
DCA-EDC mixture (55 vol-% DCA) as functions of temperature.
The values for PBLG are given in Table 4-2 and those for
PCBL are in Table 4-3. The excellent agreement of the
PBLG values with the directly estimated ones listed in the

Table 4-4. Thermodynamic parameters associated
with helix-coil transition of PBLG
and PCBL in DCA-EDC mixtures

	PBLG	PCBL
ΔH_0, cal/mol	-800	-510
ΔS_0, cal/deg mol	-1.6	-1.2
ΔH_a, cal/mol	-3500	-3100
ΔS_a, cal/deg mol	-11.4	-9.4
s_0, at 30°C	1.69	1.32
K, at 30°C	1.2	1.51

same table justifies the validity of the extrapolation procedure based on Eq. (4-18). On the other hand, the extrapolated s_L value appears to be consistently smaller than those derived from the copolymer data, which implies that the helical conformation of the block copolymer is stabler than expected from the homopolymer data alone. Thus we find that the molecular mechanism we have assumed for the boundaries between blocks is too simple to account for such stability enhancement.

4-6   Summary

Nagai's theory[22] of helix-coil transition in homopolypeptides has been extended to derive an expression for helical triblock copolypeptides of the type G-L-G. The helical fraction of the block copolypeptide was expressed as functions of s, σ, and the degree of polymerization of each block. Conformational induction by the flanking BLG blocks observed in m-cresol was illustrated successfully by the theory thus developed. Helix-coil transitions in PBLG and in block copolypeptides of BLG and CBL in DCA-EDC mixtures were investigated. The appropriate transition solvent composition of block copolypeptides was found to be about 55 vol-% DCA. The transition parameters of PBLG and the block copolypeptides

determined in a DCA-EDC mixture (55 vol-% DCA) were compared with those calculated by use of the theory proposed for the solvent effect.[30,32] The consistency between experimental values and calculated ones for PBLG was quantitative, but that for P.CBL was only qualitative.

Chapter 5

Conformation of Poly(L-Alanine) Flanked with
γ-Benzyl L-Glutamate Blocks in m-Cresol

5-1 Introduction

It is well known that the stability of α-helical
conformation of a given polypeptide depends largely on its
side chain, i.e., the kind of amino acid residue, and
solvent conditions.[1-16] Many investigations have been
performed to know about the roles that the amino acid side
chain and solvent play in determining the conformation of
polypeptides in solution. Among the polypeptides studied
so far, poly(L-alanine) (PLA) is unique and may serve as
a reference material from various points of view, because
it has only one methyl group as its side chain and very
important in the protein structure. However, PLA is
hardly soluble in ordinary organic solvents as well as in
aqueous media, and hence its conformation studies have
been possible only in such particular solvents as DCA,
hexafluoroisopropanol (HFIP), trifluoroacetic acid (TFA),
and mixtures containing these organic acids.[93-96] This
solubility problem may be solved by a technique called
"block copolymer technique", which utilizes a given
non-polar polypeptide sandwiched between blocks of

hydrophilic D,L-polypeptide. Gratzer and Doty[50] were the first to demonstrate the potential of this technique by investigating the conformation of PLA flanked with poly(D,L-glutamic acid) in aqueous solution. Since then the same procedure has been applied by subsequent investigators to PLA and other hydrophobic polypeptides.[96-103]

Motivated by these studies, we chose PLA flanked with PBLG chain in order to study the conformation of PLA in organic solvents. PBLG chosen as flanking block dissolves in many organic solvents so that it was expected to help solubilize the central chain of major concern.

Polypeptides are electrically polar, carrying permanent dipoles at the planar CO-NH groups of the backbone chain and generally at some atomic group of the side chain.[104] Because of the vector nature of dipoles, we should in principle obtain information about the mean-square dipole moment averaged over all possible conformations of the backbone and all accessible orientations of the side chain from dielectric measurements. In the α-helical conformation, a polypeptide molecule should form a large permanent dipole, since all the dipoles on the backbone chain point approximately parallel to the helix axis, whereas the side

chain dipoles almost cancel with each other due to their random orientation. We may extract information about the side chain orientation from the difference between the overall dipole moment and the backbone dipole moment if the latter can be estimated separately. Wada[104] proposed two methods for evaluating the backbone dipole; in one of them DL random copolymers of γ-benzyl glutamates were used, and in the other random copolymers of BLG and L-alanine (LA) were examined. However, both involve rather lengthy extrapolation procedures, so that the accuracy of the derived values has to be checked by some independent experiments. One of the aims of investigation in this chapter is a direct evaluation of the backbone dipole with the use of BLG-LA copolymers.

5-2   Polypeptide Samples

Triblock copolypeptides of the type BLG-LA-BLG were synthesized by successive polymerization of BLG-NCA and LA-NCA, using a procedure similar to that in Chapter 3. The only difference was that dichloromethane (DCM), instead of DMF, was used as solvent at the second and third stages of polymerization. When the LA-NCA content was large, the polymerization mixture became turbid after addition of LA-NCA at the second stage. The solution

became clearer by the addition of DCM, but remained slightly turbid for larger LA-NCA contents. This was probably because the PLA chains tended to form aggregates in DCM or DMF for their poor solubility. It seemed that the amino acid residue at the growing end of the preformed polymer maintained a polymerizing activity even in such cases, because CO_2 gas started evolving immediately after the addition of BLG-NCA to the turbid solution. Diblock and random copolymers were prepared similarly with DMF as solvent. Samples GAG-6, GAG-7, GA-11, and GA-12 synthesized in this way were purified in the following way. They were dispersed in DMF, insoluble parts were collected and freeze-dried from dioxane solutions, though only sparingly soluble. The soluble parts contained a negligible amount of polymers presumably of low molecular weights. Random copolymers GAG-8, GAG-9, and GAG-10 were fractionated by the column elution method, and appropriate middle fractions were selected for physical measurements.

Amino acid compositions of the copolypeptides were determined by elemental analysis and NMR spectra. NMR spectra of TFA solutions were recorded on a Varian XL-100 spectrometer. Chemical shift values were obtained from the reference peak of internal tetramethylsilane. The

NMR spectra were analyzed in terms of the integrated area for the alanine CH_3 peak and that of the $\gamma-CH_2$ peak of BLG.[96] Table 5-1 summarizes the preparative data. Solubility of the copolypeptides was examined for various organic liquids, with the results given in Table 5-2. It can be seen that all the samples dissolved in DCA, TFA, HFIP, and m-cresol, but samples with higher alanine contents did not dissolve in DMF, DCM, and dioxane. Sedimentation equilibrium experiments were performed to obtain weight-average molecular weights, with either DMF or HFIP as solvent. The results are given in Table 5-3.

5-3 Experimental Results

5-3-1 Optical Rotatory Dispersion

Values of the Moffitt parameter b_0 obtained for the copolypeptides in m-cresol at four temperatures are summarized in Table 5-4. One can observe that the $-b_0$ values do not show an abrupt change with temperature that would be expected for a helix-coil transition but decrease only gradually with increasing temperature. This decrease in b_0 is opposite to the one which would be predicted from the dependence of b_0 on the refractive index of solvent.[69] Some polypeptides are known to

Table 5-1. Preparative data for copolypeptides

Sample code	$[A]_0/[I]_0$	$[\eta]^c$ dl/g	$\bar{N}_v{}^d$	Yield %	LA^e mol-%	Solvent[f]
GAG-1	30-5-30	0.157	62	87	10.6	DMF
GAG-2	30-10-30	0.165	67	84	11.8	DMF
GAG-3	30-20-30	0.176	74	84	26.2	DMF
GAG-4	50-30-50	0.251	115	89	22.7	DMF + DCM
GAG-5	50-50-50	0.251	115	80	36.5	DMF + DCM
GAG-6	50-75-50	0.350	175	92	45.6	DMF + DCM
GAG-7	50-100-50	0.404	210	94	51.8	DMF + DCM
GAG-8[a]	60:10	0.172	72	87	14.1	DMF
GAG-9[a]	60:20	0.166	67	88	24.4	DMF
GAG-10[a]	100:50	0.197	85	84	35.0	DMF
GA-11[b]	100-30	0.262	120	87	23.6	DMF
GA-12[b]	100-50	0.274	130	89	30.2	DMF

a. Random copolypeptides.
b. Diblock copolypeptides.
c. Determined in DCA at 25°C.
d. Estimated from intrinsic viscosities in DCA at 25°C
   using the empirical relation shown in Figure 5-4.
e. Estimated by elemental analysis.
f. Polymerization solvents.

Table 5-2. Solubilities of copolypeptides
in various solvents

Sample code	Solvents						
	DMF	DCM	dioxane	DCA	TFA	HFIP	m-cresol
GAG-1	0	0	0	0	0	0	0
GAG-2	0	0	0	0	0	0	0
GAG-3	0[a]	0	0	0	0	0	0
GAG-4	0[a]	0	X	0	0	0	0
GAG-5	X	Δ	X	0	0	0	0
GAG-6	X	Δ	X	0	0	0	0
GAG-7	X	X	X	0	0	0	0
GAG-8	0	0	0	0	0	0	0
GAG-9	0	0	0	0	0	0	0
GAG-10	0	0	0	0	0	0	0
GA-11	X	X	X	0	0	0	0
GA-12	X	X	X	0	0	0	0

0 : soluble
Δ : slightly turbid
X : insoluble
a. Aggregation

Table 5-3. Molecular weights of BLG-LA
copolypeptides in DMF and HFIP at 25°C

Sample code	$\bar{M}_w \times 10^{-4}$	$A_2 \times 10^4$ mol ml/g^2	$\bar{N}_w$	$\bar{N}_G$	$\bar{N}_A$	LA[a] mol-%
GAG-1	1.34[b]	7.6	66.3	68.7	7.5	11.3
GAG-2	1.39[b]	8.5	69.1	60.7	8.4	12.2
GAG-3	1.33	10.0	73.3	54.6	18.7	25.5
GAG-4	2.44	6.7	131.0	101.9	29.1	22.2
GAG-5	1.89	10.5	116.4	71.7	44.7	38.4
GAG-60	2.38	8.7	154.4	86.6	67.8	43.9
GAG-70	2.26	10.3	154.1	78.8	75.3	48.9
GAG-82	1.17[b]	8.6	59.5	50.1	9.4	15.8
GAG-92	1.20[b]	8.8	64.1	50.2	13.9	21.7
GAG-102	1.73[b]	5.4	101.3	68.2	33.1	32.7
GA-110	2.2_6[c]		125	93	32	25.4
GA-120	2.2_5[c]		135	87	48	35.9

a. Estimated by elemental analysis and NMR spectra.
b. Determined in DMF.
c. Viscosity-average molecular weights calculated from
   intrinsic viscosities using the empirical relation
   shown in Figure 5-4.
A_2 = Second virial coefficient.
$\bar{N}_G$ = Average number of BLG residues.
$\bar{N}_A$ = Average number of LA residues.

Table 5-4. Moffitt parameters for BLG-LA
copolypeptides in m-cresol

| Sample code | $-b_0$ | | | |
	10°C	25°C	40°C	50°C
GAG-1	564	530	510	506
GAG-2	592	546	530	520
GAG-3	560	526	510	500
GAG-4	578	550	526	524
GAG-5	550	516	506	504
GAG-60	564	538	506	498
GAG-70	556	534	512	508
GAG-82	534	508	496	482
GAG-92	526	498	478	476
GAG-102	514	488	476	466
GA-110	569	564	534	533
GA-120	559	531	513	496

show a similar temperature dependence of b_0 in helicogenic

solvents without accompanying an appreciable

conformational transition.[60,91]

For most of the right-handed α-helical polypeptides,

b_0 is reported to be in the range between -600 and -700.

One may conclude, therefore, that the conformations of

the copolypeptides examined was not perfectly helical, because their b_0 values was found between -590 and -470. However, Matsumoto and Teramoto[60] have reported that the b_0 of PBLG in m-cresol, a typical helicogenic solvent, depends appreciably on molecular weight. Using their data,[60] we may estimate that the values of b_0 for PBLG samples having the same degrees of polymerization as the copolypeptides are about -540 ~ -580. PLA is known to exist in the right-handed α-helical conformation in the solid state,[105] in some non-aqueous solvents,[106] and in aqueous solution when blocked in copolypeptides.[50,99,100] The values of its b_0 are about -600 in aqueous solutions and somewhat larger in non-aqueous solutions.[50] Although no b_0 data are available for PLA in m-cresol, we may conclude that the conformation of the copolypeptides are essentially helical in m-cresol in the temperature range between 10 and 50°C, and that the low b_0 values observed may be due to a molecular weight dependence as found with PBLG.[60]

5-3-2   Dielectric Dispersion

   Dielectric dispersion curves were obtained for m-cresol solutions at four temperatures between 15 and 50°C. Figure 5-1 shows typical Cole-Cole plots for sample

GAG-10 (unfractionated) and GAG-102 (fractionated) in
m-cresol at 25°C. The data points fall on semicircles
whose centers are located close to $\Delta\epsilon'$ axis. As expected,
the fractionated sample is more homogeneous in molecular
weight than the unfractionated one, since the plot of the
former is closer to the Debye dispersion than is the
latter. Similar trends were found with other
fractionated samples. The root-mean-square dipole moment
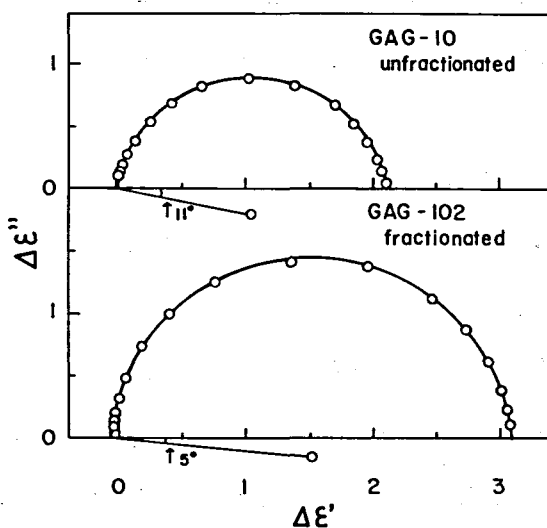$\mu = <\mu^2>^{1/2}$ and mean rotational relaxation time τ were

Figure 5-1.
Cole-Cole plots for Sample GAG-10 (unfractionated)
and Sample GAG-102 (fractionated) in m-cresol at 25°C.

estimated according to the procedure described in Chapter 3. All the numerical results are summarized in Table 5-5. It is seen that μ and τ are smooth function of temperature in the range examined. These features conform to the above-mentioned conclusion from ORD data that no conformational transition occurs in the solvent conditions studied.

Table 5-5. Dielectric dispersion data for BLG-LA
copolypeptides in m-cresol

Sample code	$\langle\mu^2\rangle^{1/2}$,D				$\tau T/\eta_0 \times 10^3$, sec deg/poise			
	15°C	25°C	40°C	50°C	15°C	25°C	40°C	50°C
GAG-1	324	328	323	322	4.10	3.90	3.76	3.58
GAG-2	337	341	341	343	4.43	4.20	4.10	3.93
GAG-3	373	375	376	369	5.21	5.10	4.79	4.72
GAG-4	640	649	648	646	19.1	18.3	17.4	16.8
GAG-5	604	608	608	615	19.1	18.7	16.8	16.7
GAG-60	820	831	832	816	40.2	39.9	37.1	34.6
GAG-70	855	861	860	858	53.5	52.5	50.0	50.7
GAG-82	292	292	296	295	3.38	3.29	3.15	3.11
GAG-92	304	301	309	304	3.89	3.91	3.42	3.50
GAG-102	539	534	523	521	11.3	10.7	9.53	9.09
GA-110	657	659	662	670	26.2	25.1	23.8	22.7
GA-120	710	721	721	712	29.2	29.3	26.9	26.1

Figure 5-2 shows molecular weight dependence of the

mean rotational relaxation times in m-cresol at 25°C

corrected for the solvent viscosity η_0 and temperature,

where the dashed line denotes the values of Matsumoto

et al.[61] for PBLG in helicogenic solvents. All the data

points, irrespective of the copolymer type, follow closely

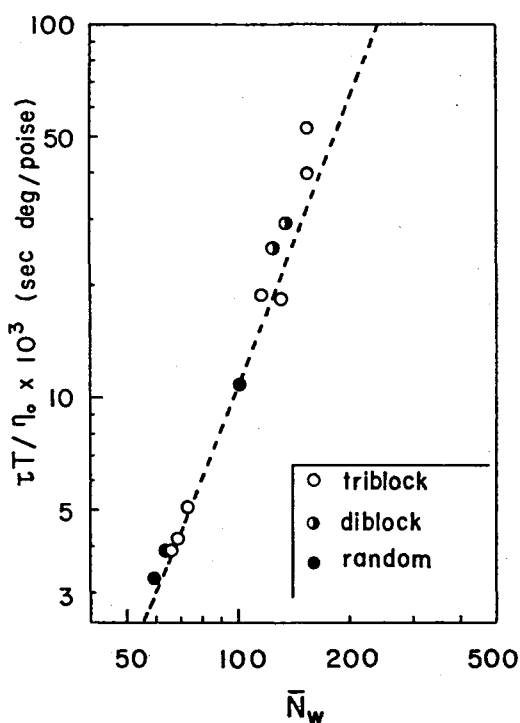the PBLG curve which has a slope of about 2.6. Ignoring

Figure 5-2.
Double logarithmic plot of $\tau T/\eta_0$ versus $\bar{N}_W$ for
copolypeptides in m-cresol at 25°C. The dashed line
denotes the data for straight rod PBLG.[61]

the difference in amino acid composition among the different samples, one can take these results to reveal that the molecular shape of the copolypeptides is straight rod. This conclusion is consistent with the finding from ORD measurements that the molecular conformation is essentially helical.

If a helical copolypeptide molecule assumes the shape of straight rod, its mean dipole moment μ may be expressed by the algebraic sum of contributions from the constituent amino acid residues, each of which is proportional to the number of the corresponding residues in the molecule. Assuming as in Chapter 3 that a certain fixed number of residues at the ends of each block end, irrespective of the total chain length, are not involved in the helical conformation, one can write for BLG-LA copolymers

$$\mu - \mu_G \bar{N}_G = (\mu^* - \mu_G \bar{N}_G^* - \mu_A \bar{N}_A^*) + \mu_A \bar{N}_A \qquad (5\text{-}1)$$

where μ_A and μ_G are the monomeric dipole moments along the helix axis of LA and BLG, respectively, and $\bar{N}_A$ and $\bar{N}_G$ are the number of LA and BLG residues, respectively. The asterisks denote the corresponding values for an arbitrary chosen reference sample.

Figure 5-3 shows a plot of $(\mu - \mu_G \bar{N}_G)$ against $\bar{N}_A$ for

triblock copolymers, diblock copolymers, and random copolymers in m-cresol at 25°C, where μ_G = 4.7 D obtained by Matsumoto et al.[61] has been used. The prediction of Eq. (5-1) is well obeyed by the data points, and the straight line yields 6.4 ± 0.1 D for μ_A. The small ordinate intercept of the line tells that the contribution from the unfolded terminal residues is negligible.
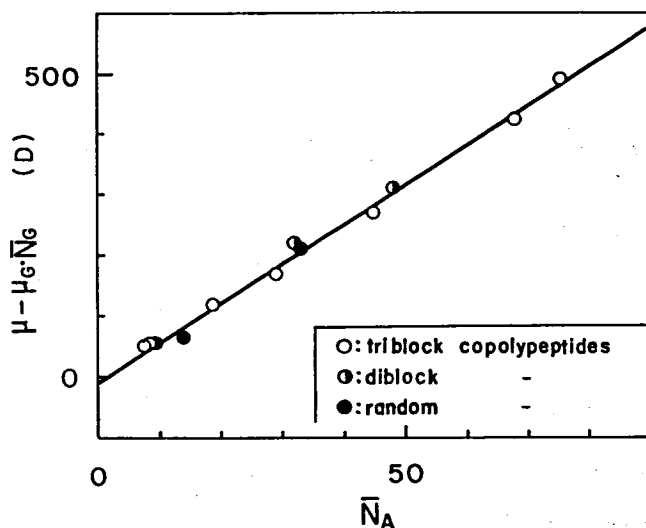
Figure 5-3.
Plot of (μ − $\mu_G \bar{N}_G$) versus $\bar{N}_A$ for copolypeptides in m-cresol at 25°C.

5-3-3 Intrinsic Viscosity

Intrinsic viscosities measured in m-cresol and DCA at 25°C are summarized in Table 5-6. Figure 5-4 shows double logarithmic plots of intrinsic viscosity versus degree of polymerization for the two solvents, where the two dashed lines represent [η] values for PBLG in DCA

Table 5-6. Viscosity data for BLG-LA copolypeptides in DCA and m-cresol at 25°C

Sample code	[η], dl/g	
	DCA	m-cresol
GAG-1	0.157	0.0710
GAG-2	0.165	0.0945
GAG-3	0.176	0.112
GAG-4	0.251	0.198
GAG-5	0.251	0.217
GAG-60	0.342	0.346
GAG-70	0.414	0.454
GAG-82	0.158	0.0773
GAG-92	0.166	0.0987
GAG-102	0.234	0.145
GA-110	0.268	0.237
GA-120	0.286	0.275

and DMF, respectively.[15,49] It is well known that for

most polypeptides DCA is a helix-breaking solvent,

whereas DMF is a helicogenic solvent. This is the case

with PBLG, too. Thus the PBLG data suggest that in this

range of small $\bar{N}_W$ [η] in a helicogenic solvent is

smaller than that in a random coil solvent. One can

observe in Figure 5-4 that the [η] in m-cresol is smaller

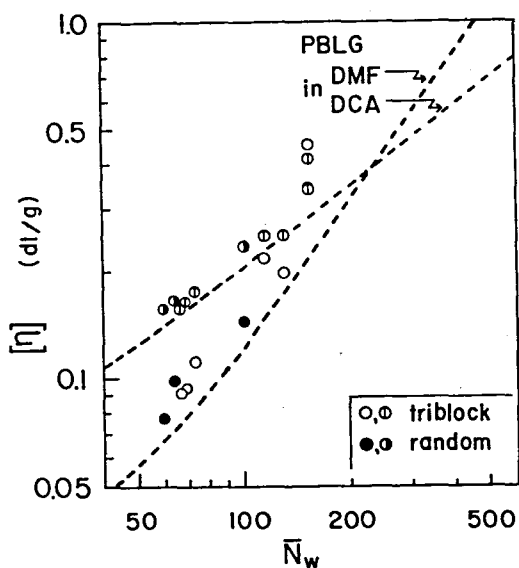than that in DCA for every sample, except for sample

Figure 5-4.
Double logarithmic plots of [η] versus $\bar{N}_W$ for BLG-LA
copolypeptides in DCA and m-cresol at 25°C. (O), (⊕),
triblock samples in m-cresol and DCA, respectively,
(●), (◑), random samples in m-cresol⌄DCA, respectively.
                                              and

GAG-70. These results may be taken to imply that the
molecular conformation is helical in m-cresol and is
randomly coiled in DCA, which is consistent with the
dielectric dispersion data and ORD data mentioned above.
However, there are arguments that the PLA molecule is
partially helical in DCA,[93,95] so that no more conclusion
than this can be extracted from the present [η] data
alone.

5-4 Discussion

When a polypeptide molecule takes up a rigid
α-helical conformation, the backbone dipoles are arranged
almost parallel to the helix axis, whereas the side chain
dipoles may undergo thermal fluctuations. The dipole
moment of a helix unit, μ_h, consists of two contributions,
one from the dipole associated with the backbone CO-NH
group and the other from the side chain dipoles located,
for example, at the C=O group. The determination of μ_h
will provide useful information about the average
orientation of the side chain relative to the helix axis.
The available data for μ_h for various polypeptides are
listed in Table 5-7, where the values deduced by Wada[104]
are also included for comparison. For each polypeptide
there is a small difference between Wada's value[104] and

Table 5-7. Comparison of monomeric dipole moments

Polypeptide	Side chain	μ_h, D Ours[d]	Wada
PLA	$-CH_3$	6.4	6.0
PBLA[a]	$-CH_2-COO-Bzl^c$	4.6	3.0
PBLG	$-(CH_2)_2-COO-Bzl$	4.7	3.4
PCBL	$-(CH_2)_4-NH-COO-Bzl$	5.4 ~ 6.2	–
PBDLG[b]	$-(CH_2)_2-COO-Bzl$	–	6.0

a. Poly(β-benzyl L-aspartate).
b. Random copolypeptide of PBLG and PBDG.
c. Benzyl group, i.e., $-CH_2-C_6H_5$.
d. Data obtained in our laboratory, i.e.,
   PLA : This work, PBLA : Saruta et al.[85]
   PBLG : Matsumoto et al.[61]
   PCBL : Omura et al.[63]

those of others.[61,63,85] This is because different
equations have been used to estimate dipole moments from
dielctric data. Therefore, the relative change in μ_h
among different polypeptides is important. One can
observe in Table 5-7 that the μ_h for PLA is larger than
those of the other polypeptides. Since alanine has no
polar side chain, its μ_h should represent the backbone
moment itself. Wada[104] had taken this trend to imply
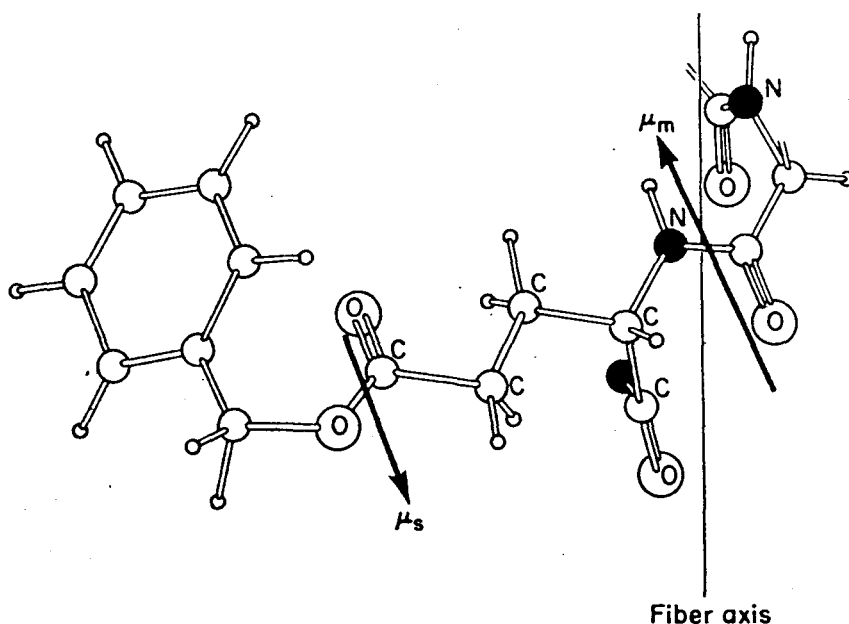
Figure 5-5.

A model for the side chain conformation of PBLG and orientation of its dipole. The side chain dipole in the CO group runs antiparallel with the backbone amide dipole; μ_m=main chain dipole, μ_s=side chain dipole.

that for a helical polypeptide with a flexible polar side chain the direction of the side chain dipoles becomes more or less antiparallel with the backbone dipole. The present result confirms his conclusion. It is worthwhile to note that Wada's conclusion[104] is compatible with a model built by Tsuboi[107] for the side chain of PBLG in the solid state on the basis of infrared dichroic spectra of oriented films (see Figure 5-5).

When a polypeptide molecule has flexible polar side

chains, the side chain dipole tends to run more or less antiparallel with the backbone dipole due to the dipole-dipole interaction between them, thus reducing the total dipole moment of the molecule. Such a trend is expected to become less pronounced as the side chain gets longer and the side chain polar group is removed from the backbone. The observed fact that μ_h is an increasing function of the side chain length is compatible with this expectation. However, Bradbury et al.[108] from the NMR shifts of the β-methylene protons of PBLG and PBLA concluded that the side chains of these polypeptides in the helical conformation had no specific orientation. Erenrich and Scheraga[84] examined the monomeric dipole moments of PBLA and its phenyl-substituted derivatives and reached a similar conclusion. Although we have no definite explanation for this discrepancy, we are tempted to consider that the NMR and dielectric dispersion might be associated with different conformational averages.

Gratzer and Doty[50] reported that the α-helix of alanine was very stable in water. On the contrary, the measurement by Ingwall et al.[100] showed that the alanine helix was not so stable. In Chapter 3, we showed that the conformational induction by flanking blocks occurs in the triblock copolypeptides of the type BLG-CBL-BLG.

Conformational induction has also been reported for DL and other types of block copolypeptides.[53,70,71] A similar effect of conformational induction must be found also with the block copolypeptides studied here, but the data are still insufficient to carry out even a qualitative analysis.

5-5   Summary

Triblock, diblock, and random copolypeptides of BLG and LA were synthesized by successive polymerization of the corresponding NCAs with initiation by n-butylamine. It was shown by ORD measurements that all the copolypeptides were essentially helical in m-cresol between 10 and 50°C. An analysis of dielectric dispersion data in m-cresol yield a value of 6.4 ± 0.1 D for the monomeric dipole moment of LA residue. This value is larger than those reported for other polypeptides, which fact is taken to mean that the side chain dipole runs antiparallel with the backbone dipole. For polypeptides carrying a polar side chain, the monomeric dipole moment tends to increase with increasing side chain length. This is ascribed to the fact that the side chain dipole may get increased rotational freedom as the side chain gets longer.

Chapter 6

Conformation of Diblock Copolypeptides of γ-Benzyl
D-Glutamate and L-Glutamate in m-Cresol

6-1 Introduction

Two methods[49,61,109] have been proposed to
synthesize a once-broken rod, one of the intermediate
conformations between random coil and rigid rod. One is
the polymerization of an N-carboxy-α-amino acid anhydride
(NCA) with a diamine as an initiator, and the other is
the block copolymerization of D and L forms of NCA. In
the former, the diamine residue incorporated somewhere in
the central part of the chain may not be torelant of
helix formation and should act as a more or less flexible
joint connecting the two helical chains. It is
experimentally established that poly(α-amino acid)
consisting of one type of enatiomorphic residues forms a
helix of one definite screw sense, e.g., poly(γ-benzyl
L-glutamate) (PBLG) forms a right-handed α-helix, whereas
the D enatiomer forms the left-handed helix.[110] In the
case of DL copolypeptide, a few monomer units located in
the boundary region between D and L chains cannot be
involved in an α-helix of one screw sense at the same
time, so they might play a role of flexible joint

connecting the two helical rods. This expectation did not always agree with the recent dielectric dispersion measurements on equimolar copolymers by Matsumoto,[111] who found that the copolymer behaved more or less like straight rods. This may be attributed either to that the boundary region has negligible flexibility or to that the entire molecule is forced to take helical conformation of one screw sense (conformational induction). Matsumoto[111] has taken the former view, but the conformational induction was actually observed for the first time by Lundberg and Doty[53] who studied DL block copolymerization of BLG and BDG. The conformational induction has also been noted for other types of block copolypeptides and random copolypeptides.[70,71,104,112-114]

In this chapter, we deal with DL block copolypeptides of different D/L mole ratios prepared by successive polymerization of BDG-NCA and BLG-NCA with the primary amine initiation. Polymerization processes and conformations in helicogenic solvents have been studied by optical rotatory dispersion, dielectric dispersion, and infrared spectroscopy to disclose the effect of conformational induction.

Table 6-1. Preparative data for diblock copolypeptides

Sample code	$[A]_0/[I]_0$	$\bar{M}_v \times 10^{-4}$ [a]	$\bar{N}_v$	BLG[b] mol-%	Yield %
DL-1	10-10	0.80	36	47.0	83
DL-2	25-25	1.29	59	47.0	91
DL-3	50-50	1.90	87	48.0	80
DL-10	20-30	1.25	57	41.4	82
DL-11	20-40	1.50	68	32.8	81
DL-12	20-80	1.80	82	19.4	87
DL-13	20-160	2.30	105	-	87
DL-16	20-5	0.60	27	7.8	73

a. Calculated from intrinsic viscosities in DCA
   at 25°C $[\eta]_{DCA}$ using the empirical relation
   between $[\eta]_{DCA}$ and $\bar{M}_w$ for PBLG.[15,49]
b. Estimated by optical rotation data in DCA at 25°C.

6-2 Polypeptide Samples

Diblock copolypeptides having a structure BLG-BDG
were obtained by successive polymerization of BLG-NCA and
BDG-NCA in DMF at room temperature according to the scheme
discribed in Chapter 2. Table 6-1 gives the preparative
data. Most of the diblock samples were fractionated by
the column elution method with methanol-DCM mixtures as

Table 6-2. Molecular weights of fractionated diblock
copolypeptides in DMF at 25°C

Sample code	$\bar{M}_W \times 10^{-4}$	$A_2 \times 10^4$ mol ml/g^2	BLG mol-%	$\bar{N}_W$	$\bar{N}_D$	$\bar{N}_L$
DL-1	0.732	19.0	47.0	33.4	17.7	15.7
DL-2	1.17	10.0	47.0	53.4	28.3	25.1
DL-032	1.-2	6.3	48.6	83.1	42.7	40.4
DL-102	1.33	10.4	36.0	60.7	38.8	21.9
DL-112	1.53	12.1	28.3	69.9	50.1	19.8
DL-123	1.74	7.7	16.7	79.5	66.2	13.3
DL-134	2.45	6.2	8.8	111.9	102.1	9.8
DL-162	0.741	11.3	9.0	33.8	30.4	3.4

$\bar{N}_L$ = the degree of polymerization of the L-block.
$\bar{N}_D$ = the degree of polymerization of the D-block.

eluents, and appropriate middle fractions of them were
used for physical measurements. The results from the
molecular weight determination are given in Table 6-2.
Here the amino acid compositions of the diblock
copolypeptides were estimated by optical rotation data
in DCA at 25°C.

6-3 Optical Rotation

6-3-1 Polymerization Process

Lundberg and Doty[53] studied the polymerization process of BDG-NCA initiated by the preformed PBLG and found that a few BDG residues attached to the L-chain were forced to assume the right-handed α-helix
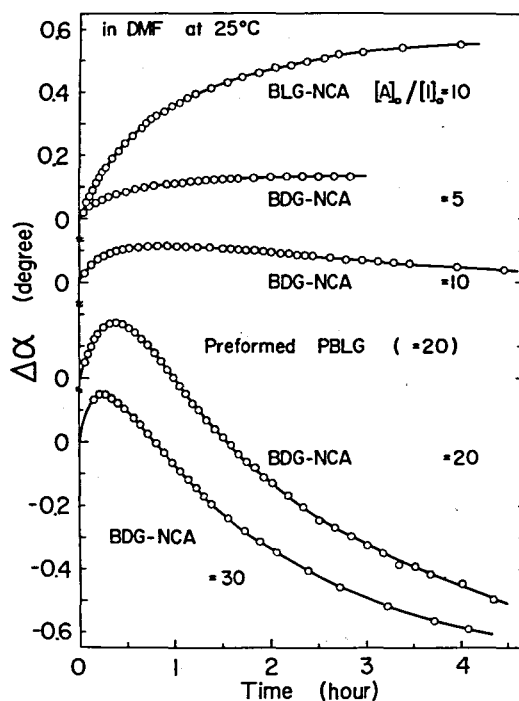

Figure 6-1.
Changes in optical rotation during the polymerization of BLG-NCA and BDG-NCA initiated by aliquots of the preformed PBLG for the $[A]_0/[I]_0$ values indicated. The value of $[A]_0/[I]_0$ of the preformed PBLG is equal to 20.

characteristic of PBLG. We performed similar experiments
to know to what extent such conformational induction
persist in copolypeptides of the types BLG-BDG and
BLG-BDG-BLG.

Figure 6-1 illustrates the change in optical
rotation,$\Delta\alpha$, accompanying the successive polymerization
of BDG-NCA and BLG-NCA initiated by aliquots of the
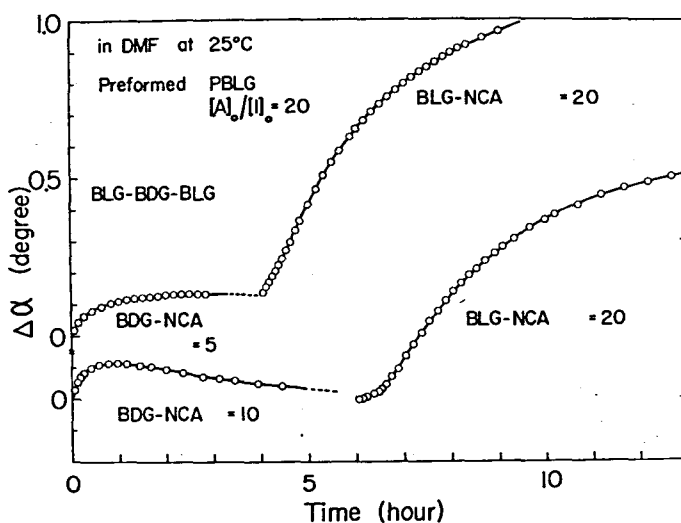preformed PBLG solution. In all the cases the initiator

Figure 6-2.
Changes in optical rotation during the polymerization
of BLG-NCA at the third stage of block copolymerization.
The value of $[A]_0/[I]_0$ at the three atages are 20-5-20
and 20-10-20, respectively.

PBLG had $[A]_0/[I]_0$ of 20, where $[A]_0$ and $[I]_0$ are the
initial molar concentrations of BLG-NCA and n-butylamine,
respectively. The same enantiomer pair shows a monotonic
increase in optical rotation, whereas the opposite pair
shows an initial increase followed by a gradual decrease
toward some plateau value. For larger BDG contents, the
helix sense eventually reverses as the polymerization
proceeds. More precisely speaking, for $[A]_0/[I]_0$ of BDG
equal to 5, the change is monotonous increase, while for
$[A]_0/[I]_0 > 10$ it exibits a distinct maximum. This
result shows that the helix sense of the attached PBLG
chain reverses at $[A]_0/[I]_0$ between 5 and 10, which
confirms the previous finding of Lundberg and Doty.[53]
Figure 6-2 illustrates how $\Delta\alpha$ changes with time in the
polymerization of BLG-BDG-BLG copolypeptides at the
indicated $[A]_0/[I]_0$ values. In both cases, the value of
$\Delta\alpha$ increases monotonously at the final stage. Thus it is
suggested that the central BDG block has been forced to
assume the right-handed α-helix by the interaction from
the flanking BLG blocks.

6-3-2 Helix-Coil Transition

    If each block of DL block copolypeptide maintains
its own helix sense, without any interaction between the

two blocks, the resulting b_0 in a helicogenic solvent
may be expressed by

$$b_0 = Xb_0^L + (1 - X)b_0^D \qquad (6-1)$$

where b_0^D and b_0^L are the b_0 values for the D and L blocks,
respectively, and X is the mole fraction of L residue;
naturally $b_0^D \approx -b_0^L$. Figure 6-3 shows a plot of b_0 versus
(1 - X) for m-cresol solution (O) and DMF solution (⊕)
at 25°C. It is seen that b_0 increases almost linearly
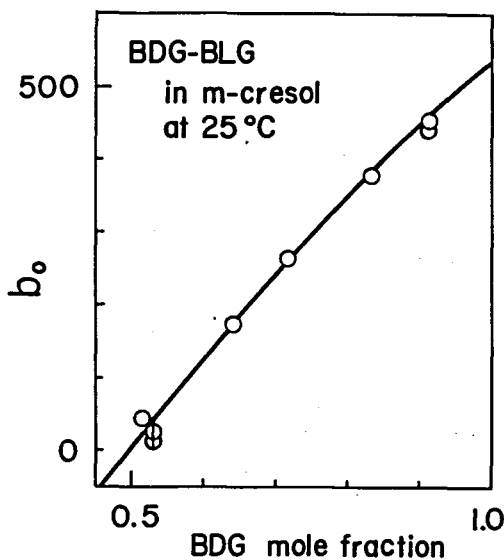
Figure6-3.
Relationship between Moffitt parameter b_0 and BDG mole
fraction for DL block copolypeptides in DMF (⊕)[111] or
m-cresol (O) at 25°C.

with (1 - X), giving about 530 at X = 0. Between 25 and 65°C, the b_0 value for either sample decreased slightly with increasing temperature but showed no sign of transition. We may conclude from these results that both the D and L blocks in the block copolymer maintain their own screw senses and no detectable conformational induction takes place between them. If the conformational induction were to exist, the data points should deviate upward from the linear relation.

Figure 6-4.
Temperature dependence of b_0 for samples DL-102 and DL-112 in a DCA-EDC mixture (55 vol-% DCA). The filled circles indicate the experimental values and the open circles are calculated by Eq. (6-1).

Figure 6-4 shows plots of b_0 versus temperature for
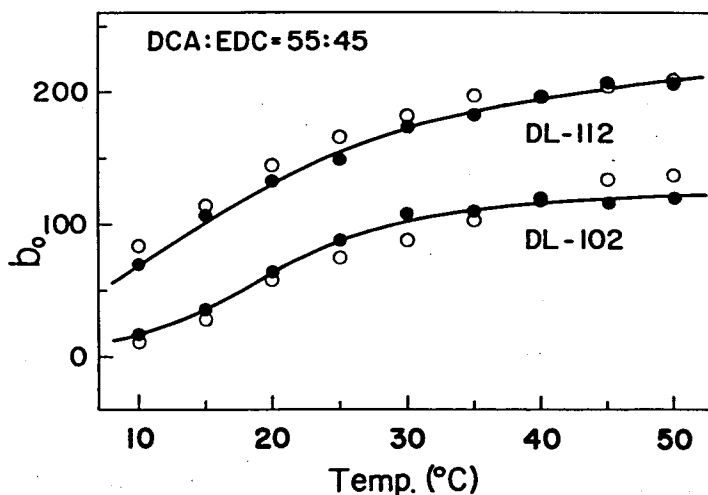samples DL-102 and DL-112 in a DCA-EDC mixture (55 vol-%
DCA) (filled circles). One can observe that the diblock
copolypeptides undergo a thermally-induced helix-coil
transition as does a low molecular weight PBLG (see
Figure 4-7 in Chapter 4). If it is assumed that the two
blocks in a diblock copolypeptide undergo the transition
independently, the observed b_0 should be equal to the
value that would be obtained for a mixture of PBLG and
PBDG of the corresponding chain lengths. The open
circles in Figure 6-4 denote the b_0 values calculated
from Eq. (6-1) on this assumption, with the b_0 values of
sample PBLG A-2, PBLG A-3, and PBDG A_n-4 being used for
b_0^L and b_0^D. Good agreement between observed and
calculated b_0 ensures the assumption that each block
undergoes a thermal transition independently.

Klug and Applequist[71] observed an appreciable
induction effect for diblock copolypeptides with shorter
D chains in helicogenic solvents. They analyzed their
b_0 data as a function of the length of D chain to estimate
the free energy difference between left-handed and right-
handed α-helices, giving 100 ~ 600 cal/ mol of res. The
reported value of the Zimm-Bragg s for PBLG (regular

-108-

right-handed helix) in m-cresol at 25°C is 1.6,[60] which

corresponds to a free energy difference of -280 cal/mol

of res. Therefore the fact that no conformational

induction was detected for higher molecular weights

suggests that the free energy difference between left-

handed and right-handed helices is at least larger than

280 cal/mol of res. For a more quantitative discussion,

one must resort to a statistical mechanical treatment of

Go and Saito,[72] in which a polypeptide chain is allowed

to assume both right-handed and left-handed helices.

However, experimental data are still insufficient to

apply it.

6-4   Infrared Spectra

Skeletal vibrations of polypeptide chains are often

conformationally sensitive and reflect small perturbations

which are caused by introducing a few D-residues in a

sequence of L-residues. Especially, the bands appearing

in the far-infrared region can be used for conformational

diagnoses of polypeptide chains and for estimating the

fraction of the α-helical forms.[115] In a random

copolypeptide of D,L-amino acids, the minor residues, say

D-residues, incorporated in long chains of L-residues

will be forced to take up the right-handed helical sense

characteristic of L-homopolypeptides.[104,112-114]

Therefore, the right-handed α-helix of the copolypeptide may be slightly deformed by the presence of the minor component and may give rise to new absorption bands which are located at different wavenumbers and have different intensities from those of the regular α-helix.

Tsuboi et al.[112] synthesized a series of copoly D,L-γ-benzyl glutamates with various D/L ratios and studied the effect of such structure deformation on infrared spectra. They interpreted the absorbed spectra changes as follows; the parallel bands at 1440 and 1422 cm^{-1}, the stronger parallel bands at 1354, 1298, and 1213 cm^{-1}, and the perpendicular band at 1212 cm^{-1} arise from the D-residues incorporated in the right-handed α-helix of PBG, and the parallel bands at 1419, 1119, and 563 cm^{-1} and the perpendicular band at 1121 cm^{-1} arise only from the regular α-helix of PBLG. In Figure 6-5 some of the absorption curves obtained with oriented films are given. For comparison the absorption curves of homopolypeptide sample PBLG-5 ($\bar{M}_v = 44 \times 10^4$) are shown. As can be seen from Figure 6-5, the spectra for the copolymers resemble very closely those of PBLG. Therefore, the fraction of deformed helix, if present, connot be estimated from these data.

Figure 6-5.

Infrared absorption spectra of oriented films of PBLG
and DL block copolypeptides in the $1000 - 1800$ cm^{-1}
region. (———) electric vector of infrared radiation
parallel to the fiber axis, (....) electric vector of
infrared radiation perpendicular to the fiber axis.

According to Tsuboi et al.[112] a DL copolypeptide

molecule in the solid state assume three different

conformations, i.e., regular α-helix, deformed helix, and

random coil. Their relative fractions may be estimated

by measuring infrared absorption intensities of

conformation-sensitive bands. The bands at 563 and 613 cm^{-1} of unoriented films were chosen for this purpose, because the former was considered to be solely due to the regular α-helix and the latter was associated with both regular and deformed helices. The intensity of the band at 697 cm^{-1} (assigned to the CH out-of-plane vibration of the benzene ring) was used as an internal standard. Sample PBDG A_n-52 was selected as the reference for the regular helix. Figure 6-6 shows
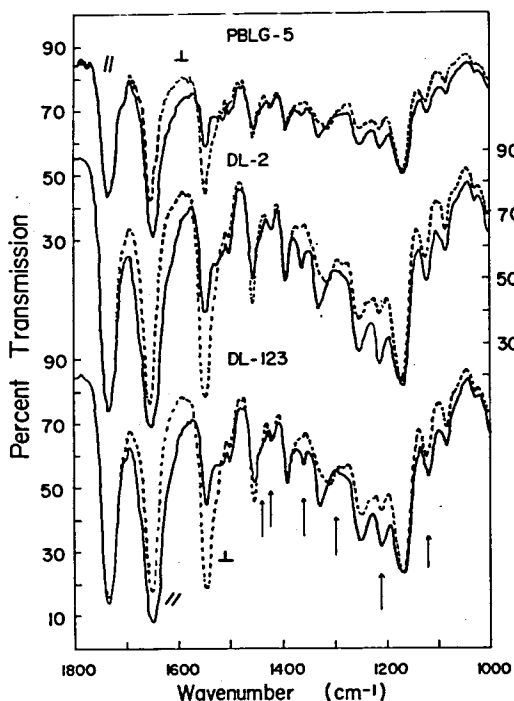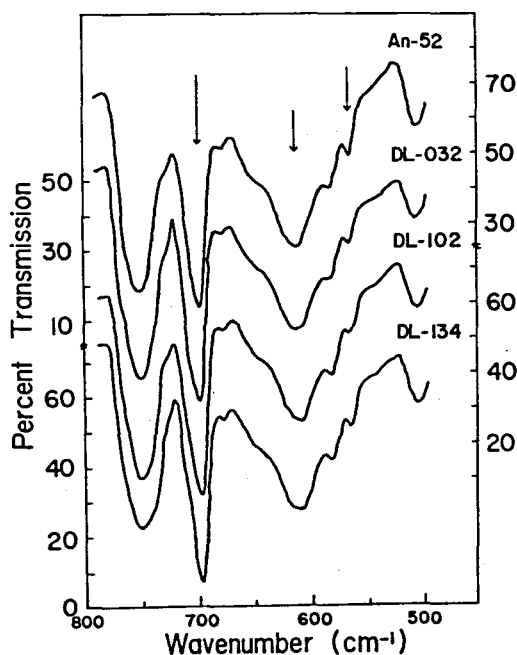

Figure 6-6.

Infrared absorption spectra of unoriented films of PBLG and DL block copolypeptides in the 800-550 cm^{-1} region.

infrared absorption spectra of unoriented films in the low wavenumber region. Table 6-3 summarizes the relative absorbances of the bands at 613 and 563 cm^{-1} and the fractions of regular and deformed helices for various samples. One can observe in Table 6-3 that, on the average, the sum of regular and deformed helices appears to be somewhat larger than the regular helix alone. However, the difference between them, i.e., the fraction of deformed helix, is not beyond the errors in the determination of absorbances. Therefore we may conclude

Table 6-3. Ratios of absorbances at 563, 613, and 697 cm^{-1}, and helical fractions

Sample code	$\dfrac{A_{613}}{A_{697}}$	$\dfrac{A_{563}}{A_{697}}$	helical fraction regular + deformed	regular
A_n-52	0.264 ± 0.02	0.127 ± 0.015	1.00	1.00
DL-1	0.152	0.062	0.58	0.49
DL-2	0.258	0.128	0.98	1.0
DL-032	0.241	0.106	0.91	0.83
DL-102	0.234	0.107	0.87	0.84
DL-112	0.250	0.113	0.95	0.89
DL-123	0.253	0.133	0.96	1.0
DL-134	0.237	0.116	0.90	0.91

that there is not appreciable conformational induction in the solid state, too. Thus we find a situation quite different from the case of random copolymers, where a considerable fraction of deformed helix has been observed.[112-114] This is probably because the conformational induction persists only over a short chain length, a fact noted in the polymerization kinetic experiments.

6-5 Dielectric Dispersion

Figure 6-7 shows typical Cole-Cole plots for samples
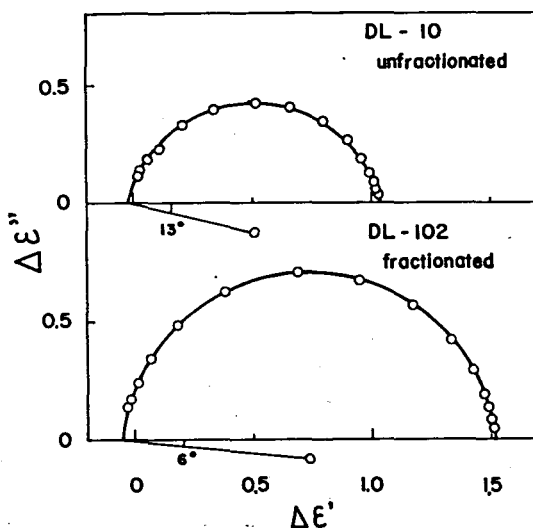
Figure 6-7.
Cole-Cole plots for samples DL-10 and DL-102 in m-cresol at 25°C.

Table 6-4. Dielectric dispersion data for diblock
copolypeptides in m-cresol at 25°C

Sample code	$\langle \mu^2 \rangle^{1/2}$ D	$\tau T/\eta_0 \times 10^3$ sec deg/poise
DL-1	134	1.23
DL-2	225	2.88
DL-032	337	6.69
DL-102	254	2.68
DL-112	285	3.75
DL-123	316	5.40
DL-134	459	11.9
DL-162	141	1.01

DL-10 (unfractionated) and DL-102 (fractionated) in
m-cresol at 25°C. The data points for each sample form a
semicircle with its center located near the Δε' axis,
which indicates that the molecular weight distributions
of both samples are moderately narrow. Similar data were
obtained for other samples. The mean-square dipole
moment and mean rotational relaxation time were calculated
by the procedure described in Chapter 3. All the
calculated results are given in Table 6-4. Figure 6-8
shows the molecular weight dependence of dipole moment,
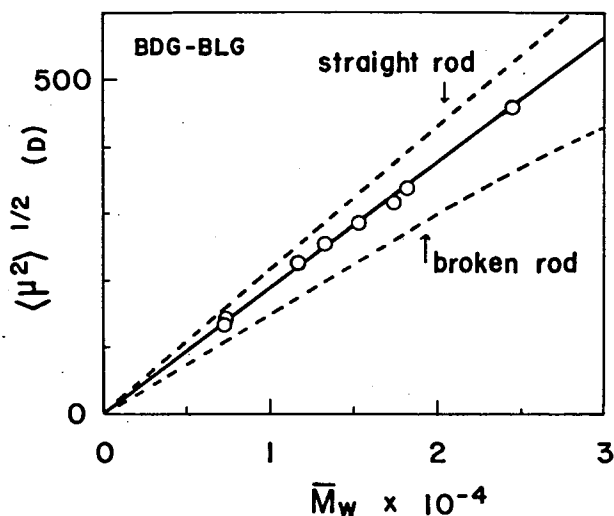
Figure 6-8.
Molecular weight dependence of dipole moment for DL
block copolypeptides. The dashed lines denote the
data for straight rod PBLG (upper) and for once-broken
rod PBLG (lower), respectively.[61]

where, for comparison, the data of Matsumoto et al.[61] for

straight rod PBLG (upper curve) and once-broken rod PBLG

(lower curve) in helicogenic solvents are included. The

copolymer data approximately follow the curve for straight

rod at low molecular weights, as also found by Matsumoto,

[111] but deviate downward at higher molecular weights. If

the molecular shape of the DL block copolymer were of

once-broken rod with the boundary portion acting as a

flexible joint, the mean dipole moment would be $2^{1/2}$

times as small as that of the straight rod of the same

length. One can see in Figure 6-8 that the data points

for the copolymers appear plotted between straight rod

and once-broken rod. This can be understood if the

boundary portion does not permit free rotation of the two

rods. A similar explanation has been offered by

Matsumoto et al.[61] to account for the data of once-broken

rod PBLG prepared by the diamine initiation. Note that

if the internal rotation at the joint is restricted the

dipole moment becomes smaller for the diamine-initiated

polymers, in which the two chains are joined in a head-

to-head fashion, and than for the DL block polymers, in

which the two chains are joined in a head-to-tail fashion.

Figure 6-9 shows double-logarithmically the

molecular weight dependence of mean rotational relaxation

time τ corrected for solvent viscosity η_0 and absolute

temperature T, where the dashed lines denote the data by

Matsumoto et al.[61] for straight rod PBLG and for once-

broken rod PBLG in helicogenic solvents, respectively.

The data points follow closely the curve for straight rod

PBLG and are located far above the curve for once-broken

rod ones. Thus the molecular shape of our DL block

copolypeptides is hydrodynamically equivalent to rigid

straight rod. This may happen if the boundary between D and
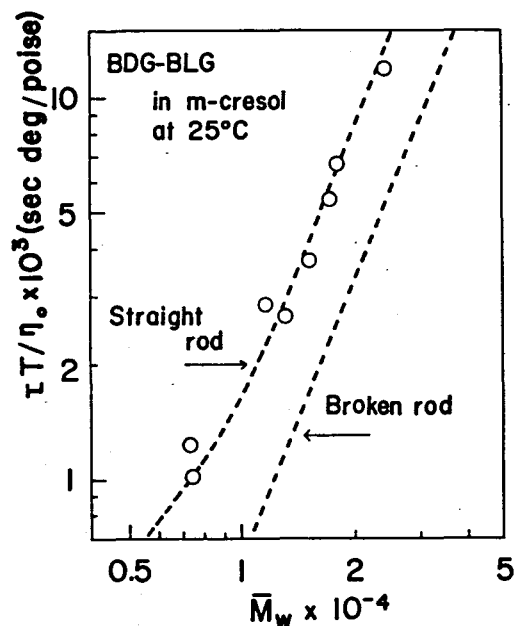
Figure 6-9.

Double logarithmic plot of $\tau T/\eta_0$ versus $\bar{M}_W$ for block copolypeptides in m-cresol at 25°C. The dashed lines denote the data for straight rod PBLG (upper) and for once-broken rod PBLG (lower), respectively.[61]

L-chains, though not in the α-helical conformation, allows a very limited internal rotation.

6-6   Intrinsic Viscosity

Intrinsic viscosities [η] in DCA and DMF at 25°C are listed in Table 6-5. Figure 6-10 shows conventional double logarithmic plots of [η] versus $\bar{M}_W$, where the two dashed lines represent the data for PBLG in DCA (upper

Table 6-5. Viscosity data for diblock
copolypeptides in DCA and DMF at 25°C

Sample code	$[\eta]$, dl/g	
	DCA	DMF
DL-1	0.104	0.0483
DL-2	0.138	0.0622
DL-032	0.180	0.0895
DL-102	0.150	0.0640
DL-112	0.163	0.0708
DL-123	0.186	0.0880
DL-134	0.231	0.125
DL-162	0.111	0.0442

curve) and in DMF (lower curve) at 25°C, respectively.[15,49]
There is no discernible difference between $[\eta]$ for PBLG
and those for the DL block copolymers. Thus we see again
that the DL block copolypeptides are hydrodynamically
indistinguishable from straight rod PBLG. This is at
variance with the experimental finding of Teramoto et
al.[109] and the theory of Yu and Stockmayer,[116] which
showed that the $[\eta]$ of a once-broken rod molecule of high
molecular weight was 0.85 times as large as that of a
straight rod of the same length. Recently Taki and
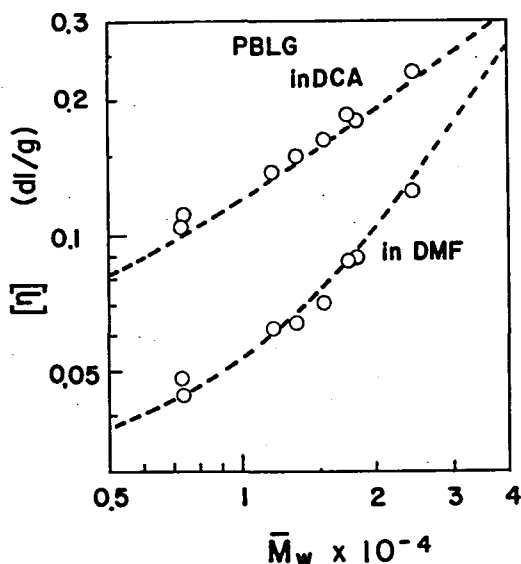
Figure 6-10.
Double logarithmic plots of [η] versus $\bar{M}_w$ for diblock
copolypeptides in DCA and DMF at 25°C, respectively.
The dashed lines denote the data for PBLG in DCA
(upper) and DMF (lower) at 25°C, respectively.[15,49]

Fujita[117] have derived theoretically even a smaller value
of 5/8 for this ratio. However, the theories are not
applicable to such low molecular weight samples as
examined in the present study.

6-7   Summary

Block copolypeptides of BLG and BDG having different
block length were synthesized by successive polymerization

of the respective NCAs with n-butylamine as initiator.
Optical rotation data and infrared spectra showed that
no conformational induction is caused in DL block
copolypeptides of relatively high molecular weights.
The molecular shape of the copolypeptides in helicogenic
solvents was found from dielectric and viscosity data to
be essentially of straight rod. These results were
explained by considering that the boundary portion
between D and L chains, though not in the helical
conformation, is subjected to a very restricted internal
rotation.

REFERENCES

1. C. H. Bamford, A. Elliott, and W. E. Hanby, Synthetic Polypeptides, Academic Press, New York, 1956.

2. H. Neurath, ed., The Proteins, 2nd edition, Academic Press, New York, 1956.

3. G. D. Fasman, ed., Poly-α-Amino Acids, Marcel Dekker, New York, 1967.

4. E. R. Blout, F. A. Bovey, M. Goodman, and N. Lotan, ed., Peptides, Polypeptides, and Proteins, Wiley, New York, 1974.

5. P. Doty, A. M. Holtzer, J. H. Bradbury, and E. R. Blout, J. Amer. Chem. Soc., 76, 4493 (1954).

6. P. Doty and J. Y. Yang, J. Amer. Chem. Soc., 78, 498 (1956).

7. P. Doty, A. Wada, J. T. Yang, and E. R. Blout, J. Polymer Sci., 23, 851 (1957).

8. P. Urnes and P. Doty, Advan. Protein Chem., 16, 401 (1961).

9. E. Katchalski and I. Steinberg, Ann. Rev. Phys. Chem., 12, 433 (1961).

10. E. Katchalski, M. Sela, H. I. Silman, and A. Berger, The Proteins, Academic Press, New York, 1965, vol. 2.

11. T. M. Birshtein and O. B. Ptitsyn, Conformations of Macromolecules, Interscience Publ., New York, 1966.

12. H. A. Scheraga, Advan. Org. Chem. Phys., $\underline{6}$, 103 (1968); Chem. Rev., $\underline{71}$, 195 (1971).

13. D. Poland and H. A. Scheraga, Theory of Helix-Coil Transitions in Biopolymers, Academic Press, New York, 1970.

14. A. Teramoto, Seibutsu-Butsuri (Japanese), $\underline{13}$, 149 (1973).

15. A. Teramoto and H. Fujita, Advan. Polymer Sci., $\underline{18}$, 65 (1975).

16. A. Teramoto and H. Fujita, to be published in J. Macromol. Sci.-Revs. Macromol. Chem.

17. B. H. Zimm and J. K. Bragg, J. Chem. Phys., $\underline{31}$, 526 (1959).

18. L. Peller, J. Phys. Chem., $\underline{63}$, 1194 (1959).

19. J. H. Gibbs and E. A. Dimargio, J. Chem. Phys., $\underline{30}$, 27 (1959).

20. A. Miyake, J. Polymer Sci., $\underline{46}$, 169 (1960).

21. S. Lifson and A. Roig, J. Chem. Phys., $\underline{34}$, 1963 (1961).

22. K. Nagai, J. Chem. Phys., $\underline{34}$, 887 (1961).

23. K. Okita, A. Teramoto, and H. Fujita, Biopolymers, $\underline{9}$, 717 (1970).

24. W. G. Miller and P. J. Flory, J. Mol. Biol., $\underline{15}$, 298 (1966).

25. M. Go, N. Saito, and M. Ochiai, J. Phys. Soc. Japan,

22, 227 (1967); M. Go and N. Saito, ibid., 28, 467
(1970).

26. M. Doi, Kobunshi (Japanese), 21, 213 (1972); M. Doi
and K. Okano, Repts. Prog. Polymer Phys. Japan, 14,
9 and 13 (1972).

27. A. Teramoto, T. Norisuye, and H. Fujita, Polymer J.,
1, 55 (1970).

28. T. Norisuye and A. Teramoto, Polymer J., 1, 341 (1970).

29. M. Bixon and S. Lifson, Biopolymers, 4, 815 (1966).

30. N. Sayama, K. Kida, T. Norisuye, A. Teramoto, and
H. Fujita, Polymer J., 1, 691 (1970).

31. T. Norisuye, K. Misumi, A. Teramoto, and H. Fujita,
Biopolymers, 12, 1533 (1973).

32. A. Maekawa, N. Nishioka, A. Teramoto, and H. Fujita,
submitted to Biopolymers.

33. S. Lifson, Biopolymers, 1, 25 (1963).

34. S. Lifson and G. Allegra, Biopolymers, 2, 65 (1964).

35. G. Allegra, J. Polymer Sci., Part C, 16, 2815 (1967).

36. D. Poland and H. A. Scheraga, Biopolymers, 7, 887
(1969).

37. G. W. Lehman and J. P. Mctague, J. Chem. Phys., 49,
3170 (1968).

38. S. S. Cohen and O. Penrose, J. Chem. Phys., 52, 5018
(1970).

39. P. H. Von Dreele, D. Poland, and H. A. Scheraga, Maromolecules, 4, 396 (1971).

40. N. Go, P. N. Lewis, M. Go, and H. A. Scheraga, Macromolecules, 4, 692 (1971).

41. P. H. Von Dreele, N. Lotan, V. S. Ananthanarayanan, R. H. Andreatta, D. Poland, and H. A. Scheraga, Macromolecules, 4, 408 (1971).

42. V. S. Ananthanarayanan, R. H. Andreatta, D. Poland, and H. A. Scheraga, Macromolecules, 4, 417 (1971).

43. K. E. B. Platzer, V. S. Ananthanarayanan, R. H. Andreatta, and H. A. Scheraga, Macromolecules, 5, 177 (1972).

44. L. J. Hughes, R. H. Andreatta, and H. A. Scheraga, Macromolecules, 5, 187 (1972).

45. J. E. Alter, G. T. Taylor, and H. A. Scheraga, Macromolecules, 5, 739 (1972).

46. H. E. Van Wart, G. T. Taylor, and H. A. Sheraga, Macromolecules, 6, 266 (1973).

47. J. E. Alter, R. H. Andreatta, G. T. Taylor, and H. A. Scheraga, Macromolecules, 6, 564 (1973).

48. L. Pauling, R. B. Corey, and H. R. Branson, Proc. Natl. Acad. Sci., 37, 205 (1951).

49. K. Nakagawa, N. Nishioka, A. Teramoto, and H. Fujita, Polymer J., 4, 332 (1973).

50. W. B. Gratzer and P. Doty, J. Amer. Chem. Soc., <u>85</u>, 1193 (1963).

51. E. R. Blout and R. H. Karlson, J. Amer. Chem. Soc., <u>78</u>, 941 (1956).

52. G. D. Fasman, M. Idelson, and E. R. Blout, J. Amer. Chem. Soc., <u>83</u>, 709 (1961).

53. R. D. Lundberg and P. Doty, J. Amer. Chem. Soc., <u>79</u>, 3961 (1957).

54. H. Fujita, Foundation of Ultracentrifugal Analysis, Wiley, New York, N. Y., 1975.

55. C. De. Loze, P. Saludjian, and A. J. Kovacs, Biopolymers, <u>2</u>, 43 (1964).

56. T. Norisuye, M. Matsuoka, A. Teramoto, and H. Fujita, Polymer J., <u>1</u>, 691 (1970).

57. M. Matsuoka, T. Norisuye, A. Teramoto, and H. Fujita, Biopolymers, <u>12</u>, 1515 (1973).

58. W. Moffitt and J. T. Yang, Proc. Natl. Acad. Sci., <u>42</u>, 596 (1956).

59. P. Doty, J. H. Bradbury, and A. M. Holtzer, J. Amer. Chem. Soc., <u>78</u>, 947 (1956).

60. T. Matsumoto and A. Teramoto, Biopolymers, <u>13</u>, 1347 (1974).

61. T. Matsumoto, N. Nishioka, A. Teramoto, and H. Fujita, Macromolecules, <u>7</u>, 824 (1974).

62. K. Nakamoto, H. Suga, S. Seki, A. Teramoto, T. Norisuye, and H. Fujita, Macromolecules, $\underline{7}$, 784 (1974).

63. I. Omura, A. Teramoto, and H. Fujita, Macromolecules, $\underline{8}$, 284 (1975).

64. T. Hayashi, S. Emi, and A. Nakajima, Polymer, $\underline{16}$, 396 (1975).

65. J. C. Mitchell, A. E. Woodward, and P. Doty, J. Amer. Chem. Soc., $\underline{79}$, 3955 (1957).

66. M. Idelson and E. R. Blout, J. Amer. Chem. Soc., $\underline{79}$, 3948 (1957).

67. M. Szwarc, Advan. Polymer Sci., $\underline{4}$, 1 (1965).

68. Y. Imanishi, Kobunshi (Japanese), $\underline{21}$, 32 and 92 (1972).

69. J. Y. Cassim and E. W. Taylor, Biophys. J., $\underline{5}$, 553 (1965).

70. L. Palillo, P. Temussi, E. Trivellone, E. M. Bradbury, and C. Crane-Robinson, Biopolymers, $\underline{10}$, 2555 (1971).

71. T. L. Klug and J. Applequist, Biopolymers, $\underline{13}$, 1317 (1974).

72. M. Go and N. Saito, J. Phys. Soc. Japan, $\underline{20}$, 1686 (1964).

73. T. Ooi, R. A. Scott, G. Vanderkooi, and H. A. Scheraga, J. Chem. Phys., $\underline{46}$, 4410 (1967).

74. A. Wada, Bull. Chem. Soc. Japan, $\underline{33}$, 822 (1960).

75. A. Wada, J. Chem. Phys., $\underline{31}$, 495 (1959).

76. A. Wada. Polyamino Acids, Polypeptides, and Proteins, M. A. Stahmann, ed., University of Wisconsin Press, Madison, WIs., 1962.

77. A. Wada and H. Kihara, Polymer J., $\underline{3}$, 482 (1972).

78. H. Kihara, K. Tanno, and A. Wada, Polymer J., $\underline{5}$, 324 (1973).

79. J. Applequist and T. G. Mahr, J. Amer. Chem. Soc., $\underline{88}$, 5419 (1966).

80. E. Marchal, C. Hornick, and H. Benoit, J. Chim. Phys. Physicochim. Biol., $\underline{64}$, 515 (1967).

81. E. Marchal and J. Marchal, J. Chim. Phys. Physicochim. Biol., $\underline{64}$, 1607 (1967).

82. H. Block, E. F. Hayes, and A. M. North, Trans. Faraday Soc., $\underline{66}$, 1095 (1970).

83. M. Sharp, J. Chem. Soc. A, 1596 (1970).

84. E. H. Erenruch and H. A. Scheraga, Macromolecules, $\underline{5}$, 746 (1972).

85. S. Saruta, Y. Einaga, A. Teramoto, and H. Fujita, to be published.

86. A. D. Buckingham, Aust. J. Chem., $\underline{6}$, 93 and 323 (1952).

87. D. C. Lee, I. Omura, S. Itou, A. Teramoto, and H. Fujita, to be published in Polymer.

88. D. C. Lee, S. Itou, A. Teramoto, and H. Fujita, to be published.

89. R. W. Woody and I. Tinoco Jr., J. Chem. Phys., 46, 4927 (1967).

90. J. N. Vournakis, J. F. Yan, and H. A. Scheraga, Biopolymers, 6, 1531 (1968).

91. J. S. Franzen, J. B. Horry, and C. Bobik, Biopolymers, 5, 193 (1967).

92. S. Saruta, Y. Einaga, A. Teramoto, and H. Fujita, to be published.

93. R. Sakamoto and Y. Okamoto, Nippon Kagaku Zasshi, 90, 753 (1969).

94. J. R. Parrish, Jr., and E. R. Blout, Biopolymers, 11, 1001 (1972).

95. A. Nakajima and M. Murakami, Biopolymers, 11, 1295 (1972).

96. E. M. Bradbury, P. D. Cary, and C. Crane-Robinson, Macromolecules, 5, 581 (1972).

97. H. J. Sage and G. D. Fasman, Biochemistry, 5, 286 (1966).

98. H. E. Auer and P. Doty, 5, 1708 and 1716 (1966).

99. N. Lotan, A. Berger, E. Katchalski, R. T. Ingwall, and H. A. Scheraga, Biopolymers, 6, 331 (1968).

100. R. T. Ingwall, H. A. Scheraga, N. Lotan, A. Berger, and E. Katchalski, Biopolymers, 6, 331 (1968).

101. R. F. Epand and H. A. Scheraga, Biopolymers, 6, 1551

(1968).

102. S. E. Ostroy, N. Lotan, R. T. Ingwall, and H. A.
Scheraga, Biopolymers, 9, 749 (1970).

103. T. Iio, Biopolymers, 10, 1583 (1971).

104. A. Wada, in Poly-α-Amino Acids, (G. D. Fasman, ed.),
Marcel Dekker, New York, 1967, Chapter 9.

105. A. Elliott and B. R. Malcolm, Proc. Roy. Soc. (London),
A249, 30 (1959).

106. A. R. Downie, A. Elliott, W. E. Hanby, and B. R.
Malcolm, Proc. Roy. Soc. (London), A242, 325 (1957).

107. M. Tsuboi, J. Polymer Sci., 59, 139 (1962).

108. E. M. Bradbury, B. G. Carpenter, C. Crane-Robinson,
and H. Goldman, Macromolecules, 4, 557 (1971).

109. A. Teramoto, Y. Yamashita, and H. Fujita, J. Chem.
Phys., 46, 1919 (1967).

110. A. Elliott, in Poly-α-Amino Acid, (G. D. Fasman ed.),
Marcel Dekker, New York, 1967, Chapter 1.

111. T. Matsumoto, unpublished data.

112. M. Tsuboi, Y. Mitsui, A. Wada, T. Miyazawa, and N.
Nagashima, Biopolymers, 1, 297 (1967).

113. S. Yamashita, Ph. D. Thesis, Osaka Univ., (1971).

114. S. Yamashita, K. Waka, N. Yamawaki, and H. Tani,
Macromolecules, 7, 410 (1974).

115. T. Miyazawa, in Poly-α-Amino Acid, (G. D. Fasman ed.),
     Marcel Dekker, New York, 1967, Chapter 2.

116. H. Yu and W. H. Stockmayer, J. Chem. Phys.,
     $\underline{47}$, 1369 (1967).

117. N. Taki and H. Fujita, Polymer J., $\underline{7}$, 637 (1975).

List of Publications of N. Nishioka

1. Excluded-Volume Effects in Dilute Polymer Solutions.
   IV. Polyisobutylene, T. Matsumoto, N. Nishioka, and
   H. Fujita, J. Polymer Sci., Part A-2, $\underline{10}$, 23 (1972).

2. Solution Properties of Synthetic Polypeptides. XIV.
   Synthesis and Characterization of Broken-Rod
   Polypeptides, K. Nakagawa, N. Nishioka, A. Teramoto,
   and H. Fujita, Polymer J., $\underline{4}$, 332 (1973).

3. Dielectric Dispersion of Polypeptide Solutions. I.
   Once-Broken Rod Polypeptide Based on γ-Benzyl
   L-Glutamate, T. Matsumoto, N. Nishioka, A. Teramoto,
   and H. Fujita, Macromolecules, $\underline{7}$, 824 (1974).

4. Conformation of Block Copolypeptides of γ-Benzyl
   L-Glutamate and ε-Carbobenzoxy L-Lysine in m-Cresol,
   N. Nishioka, A. Teramoto, and H. Fujita, Polymer J.,
   $\underline{8}$, 121 (1975).

5. Conformation of Poly(L-Alanine) Flanked with γ-Benzyl
   L-Glutamate Blocks in m-Cresol, N. Nishioka,
   H. Mishima, A. Teramato, and H. Fujita, Polymer
   Preprints, Japan, Vol. 25, No. 6, 1097 (1976).

6. Solution Properties of Synthetic Polypeptides. XXI.
   Solvent Effect on the Helix-Coil Transition of
   Poly(ε-Carbobenzoxy L-Lysine), A. Maekawa, N. Nishioka,

A. Teramoto, and H. Fujita, Biopolymers

(in preparation).

7. Helix-Coil Transition of Block Copolypeptides of
    γ-Benzyl L-Glutamate and ε-Carbobenzoxy L-Lysine,
    N. Nishioka, A. Teramoto, and H. Fujita, Polymer J.,
    (in preparation).

8. Conformation of Diblock Copolypeptides of γ-Benzyl
    D-Glutamate and L-Glutamate in m-Cresol, N. Nishioka,
    A. Teramoto, and H. Fujita, Polymer J.,
    (in preparation).